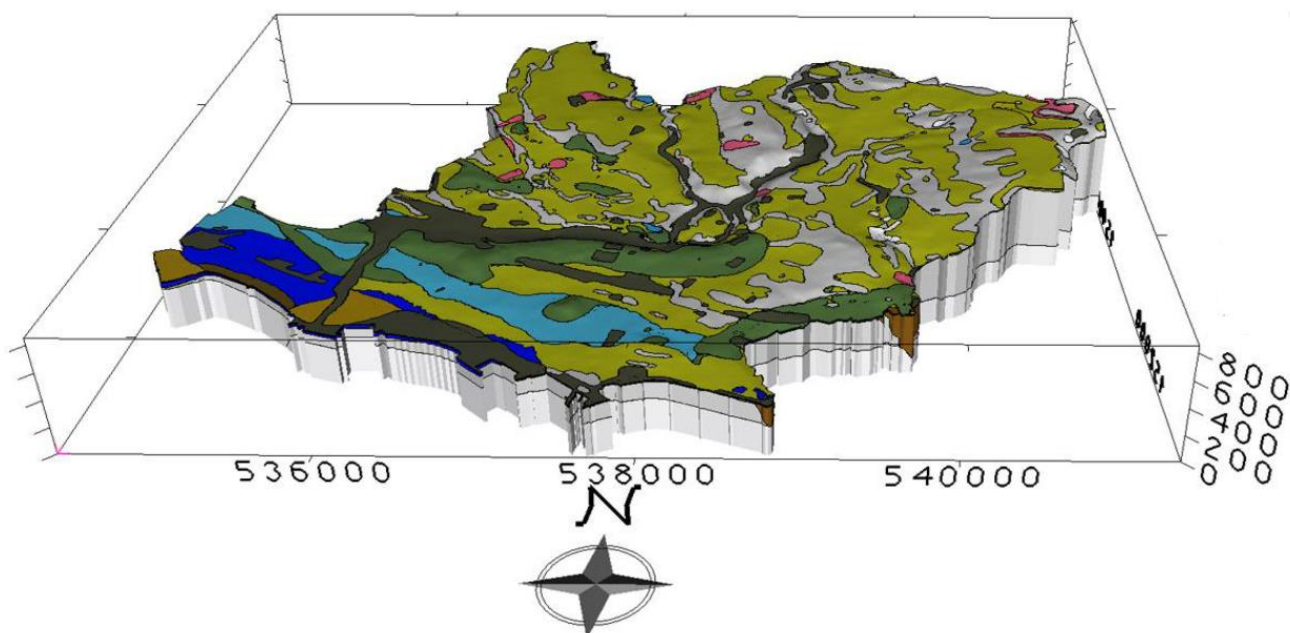


# Geotherm<sup>2</sup>



Progress Report 2014

**Project Coordinator: Prof. Stefan Wiemer**



## Impressum

### **Publisher**

Schweizerische Erdbebendienst an der ETH Zürich

### **Autors**

Dr. Peter Bayer (Engineering Geology/Geological Institute; ETH-Zürich)  
Dr. Peter Burgherr (Laboratory for Energy Systems Analysis ; Paul Scherrer Institut )  
Dr. Thomas Driesner (Institut für Geochemie und Petrologie; ETH-Zürich)  
Dr. Keith Evans (Engineering Geology/Geological Institute; ETH-Zürich)  
Prof. Dr. Patrick Jenny (Institut für Fluidodynamik ; ETH-Zürich)  
Prof. Dr. François Maréchal (Laboratoire d'énergétique industrielle; EPF-Lausanne)  
Dr. Michael Stauffacher (Institute for Environmental Decisions; ETH-Zurich)  
Dr. Laurent Tacher (Soil Mechanics Laboratory; EPF-Lausanne)  
Prof. Stefan Wiemer (Swiss Seismological Service)  
Dr. Alba Zappone (Swiss Seismological Service)

### **Compilation and Layout**

Dr. Alba Zappone (Swiss Seismological Service)

### **Cover Picture**

Lausanne shallow geological model (see Figure 13 in text)

---

## Summary

GEO THERM-2 conducts cross-disciplinary research towards the development of Enhanced Geothermal Systems (EGS). EGS is a technology that will allow the heat resources residing at several kilometers depths to be exploited for electricity and heat production. At present, EGS technology is not mature; two of the key challenges are the difficulty of (1) engineering a lasting heat exchanger with appropriate properties within deep, hot, low-porosity rocks, and (2) the risk of inducing felt and potentially hazardous seismic events during the development and operation of the heat exchanger.

GEO THERM-2 continues the work initiated in the GEO THERM-1 project (2009-2012). The project was conceived in order to provide a bridge to a major nationwide project in geothermal energy, the Swiss Competence Center Energy Research-Supply of Energy (SCCER-SoE), which was in its planning phase when GEO THERM-2 was proposed, and has begun in the meantime. GEO THERM-2 started in May of 2013, and will end in April 2016. This report describes the research activities in the time interval February 2014-November 2014.

GEO THERM-2 is a collaborative scientific project funded by the Competence Center Environment Sustainability (CCES), the Competence Center Energy and Mobility (CCEM) and the Bundesamt Für Energie (BFE), with considerable synergies and cooperation with the recently established SCCER-SoE. The collaboration of GEO THERM-2 with industrial stakeholders (Axpo, GeoEnergy Suisse) is realized through the close cooperation of GEO THERM-2 with SCCER-SoE.

The partners of the project are members of various Departments and Institutes in ETH and in EPFL, and of the Paul Scherrer Institute:

- ETH:
  - o Department of Earth sciences (ERDW):
    - Geological Institute (GI); PI: Keith Evans
    - Institute of Geophysics (IG); PI: Domenico Giardini
    - Institute of Geochemistry and Petrology (IGP); PI: Thomas Driesner
    - Swiss Seismological Survey (SED); PI: Stefan Wiemer
  - o Department of Mechanical and Process Engineering (MAVT):
    - Institute of Fluid Dynamics (IFD); PI: Patrik Jenny
  - o Department of Environmental Systems Science (USYS):
    - Institute for Environmental Decisions (IED); PI: Michael Stauffacher
- EPFL:
  - o School of Engineering
    - The Civil Engineering Institute; Laboratory of Soil mechanics (LMS); PI: Lyess Laloui
    - Institute of Mechanical Engineering; Industrial Energy Systems Laboratory (IPESE); PI: Francois Maréchal
- Paul Scherrer Institute (PSI):
  - o Laboratory for Energy Systems Analysis, Technology Assessment group (TA); PI: Peter Burgherr.

In total, thirty-eight co-workers contribute either full-time or part-time to the project, under the guidance of six professors, one of which, Prof. Stefan Wiemer, has the leadership of the whole project. The great majority of the partners of GEO THERM-2 is also involved as principal investigator or as co-worker in SCCER\_SoE, thus assuring coordination with the national - wide research programme on geothermal energy.

The main strength of GEO THERM-2 is to adopt a cross-disciplinary approach to the challenges mentioned above. The contributions of GEO THERM-2 in terms of scientific results, capacity building and knowledge transfer are a therefore critical intermediate step towards successful future Pilot and Demonstration projects, and complement the activities conducted in SCCER-SoE.

The research activities in GEOTHERM-2 are organized in six Modules, or work packages, which are designed to:

- Develop and test novel observational tools for the geomechanics of reservoir creation (Module 1: EGS reservoir characterization and geomechanics);
- Assess and mitigate the risks associated with noticeable induced seismicity (Module 2: Induced seismicity: Monitoring, risk assessment and management);
- Assess potential accidental risks leading to health and environmental impacts as well as public perceptions of risks associated with geothermal energy development (Module 3: Comparative assessment of accidental risks and social acceptance);
- Expand a multi-scale – multi-process modeling code for simulating the process of reservoir generation as well as the longer-term evolution of the reservoir during production (Module 4: A 3-dimensional H-T-M-coupled simulator for EGS reservoir creation and production);
- Investigate the effects of chemical reaction between fluid and rock on long-term permeability evolution and heat extraction from the reservoir (Module 5: Geochemical effects on long-term permeability evolution & heat extraction);
- Design a decision-support tool for optimizing the use of geothermal energy in cities, by quantifying all interacting factors including geological and economic parameters, conversion efficiency and temporal heat storage, complementary energy sources and societal acceptance (Module 6: Geothermal energy usage in cities).

The research results, the deliverables and the milestones accomplished by each module are described in detail in the following chapters. A report on the timeline and a list of available publications is also reported for each module.

In overview, the project does not suffer any significant delay from the original schedule described in the proposal. Nevertheless, the long time interval between the proposal submission and the actual start of the project has generated a few noticeable deviations from the research plan, especially within Module 2, where a few tasks have been completed well ahead the date foreseen in the time plan (Task2.3b and 2.5), while other tasks have been picked up and expanded in order to answer to new challenges arising from, for example, the induced seismicity related to the St. Gallen Project (Task 2.1 a).

The coordination across modules is guaranteed through semi-annual project meetings, hosted by different partners institutions on the basis of a rotational concept. In the reported period, a one-day semi-annual meeting was held at EPFL in July. The meeting was attended by ca. 25 participants. Furthermore, two representatives of the City of Lausanne were present at the meeting as observers. The next semi-annual meeting will be held in February at ETH Zurich in the Department of Earth Science (D-ERDW).

A Document Management System (DMS) has been designed and implemented, and is used as an information exchange intranet for the participants of GEOTHERM-2 ([dms.seismo.ethz.ch](http://dms.seismo.ethz.ch)). In this environment, presentations, publications and reports are constantly uploaded and made available to the GEOTHERM2 community. A blog has been established and is hosted under <http://leniblogs.epfl.ch/GEOTHERM-2/>, it hosts regularly meeting of the PhD-PostDoc working group.

In terms of outreach and dissemination, a GEOTHERM-2 website, hosted at the CCES website, is constantly maintained and updated. Links with relevant publication are available there. On 26 February 2014 Prof. Dr. Stefan Wiemer and Stefano Moret presented the activities of GEOTHERM-2 to the CCES community during the CCES Conference 2014 'Research, Education, and Dialogue for Environment and Sustainability – Achievements and Challenges', ETH Zurich. The review panel formulated a very favourable judgement of the activities on the project.

Prof. Wiemer met representatives of the Institute of Behavioural Sciences (Department of Humanities, Social and Political Sciences - GESS) at the beginning of March with the aim to identify themes within GEOTHERM-2 that could be of central interest for teaching activities in Physics, Chemistry and Mathematics). Numerous subjects within geothermal energy are interesting starting points in the field of thermodynamics (heat transfer in the rocks, energy changes with changes of States of matter, energy

transformations, use of temperature difference by heat pumps, etc.). We plan to dedicate a 20% full time equivalent dedicated within the next year to the creation of teaching materials (write texts, develop pre- and post- tests, tests in the classroom).

---

## Table of Content

<b>1.</b>	<b>EGS reservoir characterization and geomechanics (Module 1)</b>	<b>1</b>
1.1	Main scientific achievements and deliverables	1
1.1.1	Power spectra of stress orientation and magnitude variations for Soultz and Basel wells (Task 1.2a)	1
1.1.2	Modeling of fracture control of stress heterogeneity (Task 1.2b)	2
1.1.3	Assessment of thermal stimulation data and procedures used in Iceland (Task 1.3a)	4
1.1.4	Modeling of the thermal stimulation process (Task 1.3b)	4
<b>2.</b>	<b>Induced seismicity: Monitoring, risk assessment and management (Module 2)</b>	<b>6</b>
2.1	Main scientific achievements and deliverables	6
2.1.1	Database of injections (Task 2.1a)	6
2.1.2	Sensitivity of Mmax (Task 2.1b)	7
2.1.3	Monte Carlo style simulation of the reservoir response (Task 2.2a)	7
2.1.4	Data-mining based on a range of sequences (Task 2.2b)	8
2.1.5	Velocity tomography applied to the Basel reservoir (Task 2.3a)	9
2.1.6	Noise tomography applied To the Basel reservoir (Task 2.3b)	9
2.1.7	Imaging using migration based techniques (Task 2.4)	9
2.1.8	Spatio-temporal failure of microseismic structures (Task 2.5)	9
<b>3.</b>	<b>Comparative assessment of accidental risks and social acceptance (Module 3)</b>	<b>12</b>
3.1	Main scientific achievements and deliverables	12
3.1.1	Systematic overview of geothermal risks (Task 3.1)	12
3.1.2	Risk indicator establishment (Task 3.2)	15
3.1.3	Concept for public and stakeholder involvement (Task 3.3)	15
<b>4.</b>	<b>A 3-dimensional H-T-M-coupled simulator for EGS reservoir creation and production (Module 4)</b>	<b>18</b>
4.1	Main scientific achievements and deliverables	18
4.1.1	Simulator development (Task 4.1)	18
4.1.2	Simulator development: implementation of near-wellbore non-Darcy flow (Task 4.1a)	19
4.1.3	Simulator development: implementation of geomechanics into the simulator (Task 4.1b-d)	19
<b>5.</b>	<b>Geochemical effects on long-term permeability evolution &amp; heat extraction (Module 5)</b>	<b>23</b>
5.1	Main scientific achievements and deliverables	23
5.1.1	Code Modification and Small Scale Reactive Transport Simulation (Tasks 5.1a, 5.1b)	24
<b>6.</b>	<b>Geothermal energy usage in cities (Module 6)</b>	<b>26</b>
6.1	Main scientific achievements and deliverables	26
6.1.1	Characterization of energy services in cities (Task 6.1)	27
6.1.2	Characterization of the geothermal resources, of the cold source and possible shallow storage (Tasks 6.2 & 6.3)	28
6.1.3	Energy conversion systems (Task 6.4)	30
6.1.4	Environmental impact assessment(Task 6.5)	31
6.1.5	Energy system design(Task 6.6)	34



We derived estimates for SHmax by analyzing breakout width data from an acoustic televiewer log run the 5 km deep borehole BS-1. Some 81% of the borehole below the granite top at 2.42 km is affected by breakouts, which is favorable for examining the depth trends of the estimates. A primary objective of the analysis was to evaluate the impact of four different failure criteria on the SHmax magnitude estimates. The criteria used were Rankine, Mohr-Coulomb, Mogi-Coulomb, and Hoek-Brown 3D. All were parameterized using strength data from a single multi-stage triaxial compressive test on a core plug taken from near the well bottom. A numerical approach was employed to derive SHmax magnitude from the estimated breakout widths, taking into account all stress components at the borehole wall including the remnant thermal stress arising from the cooling of the borehole wall by the drilling. Previous studies of breakout width have shown that large, small-scale fluctuations are associated with fractures, which reflect variations in strength or stress, or both. At larger scales, breakout width tends to decrease with depth. Assuming there is no significant systematic change in the strength characteristics of the rock along the length of the hole, for which there is no evidence, the large-scale trend has the consequence of implying a small gradient of the SHmax profile. This result is independent of the failure criterion, and also of the profile of Shmin used in the analysis. The absolute values of SHmax depend upon the failure criterion used. Criteria that consider the strengthening effect of the intermediate stress (Mogi-Coulomb and Hoek-Brown 3D) yield profiles that violate frictional limits on the strength of the crust above 4 km, whereas the profiles of the Mohr-Coulomb and Rankine criteria do not (the latter two are essentially identical for the case where pore pressure and wellbore pressure are equal and in the range of Shmin and SHmax relevant for our analyses). The Mohr-Coulomb/Rankine criteria profiles indicate a trend in SHmax from favoring strike-slip faulting above 4200 m to strike-slip/normal faulting below. This is reasonably consistent with focal mechanisms recorded during the reservoir stimulation, which show a mix of strike-slip and normal faulting throughout the considered depth range.

In a paper presented at the EUROCK-2014 conference, we examined approaches for defining the scaling of stress variations along boreholes. Previous work suggested that this variability follows self-affine scaling and could be related to scaling characteristics of the natural fractures network and earthquake magnitude-frequency statistic. If this were the case, then the measurable variations in stress orientation could be used to constrain statistical attributes of the fracture network and to anticipate the seismic response of a rock mass. It is thus important to identify a robust method for estimating the scaling characteristics of the in-situ stress variations. To that end, we evaluated seven techniques for estimating the fractal dimension,  $D$ , of synthetic data series of known fractal dimension. Particular attention was given to assess the biases introduced by the presence of gaps and noise, which are invariably present in the real data. The techniques were then applied to real wellbore failure data from Soultz-sous-Forêts and Basel geothermal projects. Preliminary results indicate that significantly different estimates of  $D$  were found for different methods applied to the same dataset, which are best explained as reflecting the impact of gaps in the data. This work is on-going.

### **1.1.2 Modeling of fracture control of stress heterogeneity (Task 1.2b)**

The characteristics of fracture networks play a primary role in the creation and operation of deep geothermal reservoirs. Thus, the development of a geological model of the reservoir is a prerequisite for geomechanical simulation of the reservoir creation process. The geological model describes the spatial distribution and scaling of discontinuities within the reservoir as well as lithological variations. This task is concerned with the development of the geological model, and has two complementary components.

The first component seeks to develop methodologies for constructing a discontinuity model of a reservoir from sparse data using the Basel reservoir as a test case. In a paper accepted for the 2015 World Geothermal Congress, we analysed logging data from the 5 km deep well, Basel-1, located in Switzerland to investigate the natural fractures and zones characterised by high fracture frequency in the crystalline basement. The logs extend from 2.6 km depth, about 100 m below the weathered palaeo-surface of the granite, to a depth of 5.0 km, and include acoustic televiewer (UBI), density and p-wave velocity. The results of drill cuttings analysis were also available. Two previous analyses of the UBI log have been made. Considerable differences in the distributions of natural fractures in the crystalline basement were found from the three analyses. The differences in large part reflect the difficulty in distinguishing natural from drilling-induced fractures. Poor quality images in the open-hole section below 4.7 km resulting from stick-slip motion of the UBI probe were radically improved by applying a novel correction method using



accelerometer data. This led to fewer natural fractures in the open section than recognized in earlier studies. Fracture frequency decreases with depth from 3.1 fractures/m near the top of the logged section to 0.3 fractures/m below 3.0 km. Orientation cluster analyses revealed a complex pattern of up to 6 potential fracture sets along the well, some of which may be conjugate pairs (Figure 1). Only set 1 (steeply dipping to W–SW) is present along the entire imaged borehole, the other sets occurring over limited sections of the hole. The mean orientation of set 1 does not coincide with prominent NNE-striking Rhenish lineaments (faults) of first- and second-order in the Basel area, but strikes sub parallel to the maximum principal horizontal stress. Fractures belonging to set 1 are spatially clustered and form localized zones of high fracture frequency. Zone lengths ranged up to 100 m, but were more typically tens of meters, and below 4.0 km the zones consisted predominantly of fractures belonging to set 1. Zones of high fracture frequency did not necessarily coincide with low density or low p-wave velocity anomalies, as might be expected from fracture zones with dam-age or higher porosity.

The logging data provides high-quality information on discontinuities that intersect the well. On-going work seeks to better constrain the fracture network model of the Basel reservoir by including information from the pattern of microseismicity. Current work is focusing on the inference of fault orientations by fitting planes to clusters of microseismic events that all produce similar waveforms on seismic recording stations. Because of the high degree of waveform similarity, the events must lie close to each other and involve similar slip direction on similarly-oriented failure planes. It is assumed that the events within a cluster lie on one plane. Errors in the relative locations of events within a cluster are taken into account when determining the range of fault plane orientations that fit the relative location data. The objective is to derive the distribution of seismically-active planes within the reservoir, which can be compared with the distributions of the orientations of fractures observed in the well.

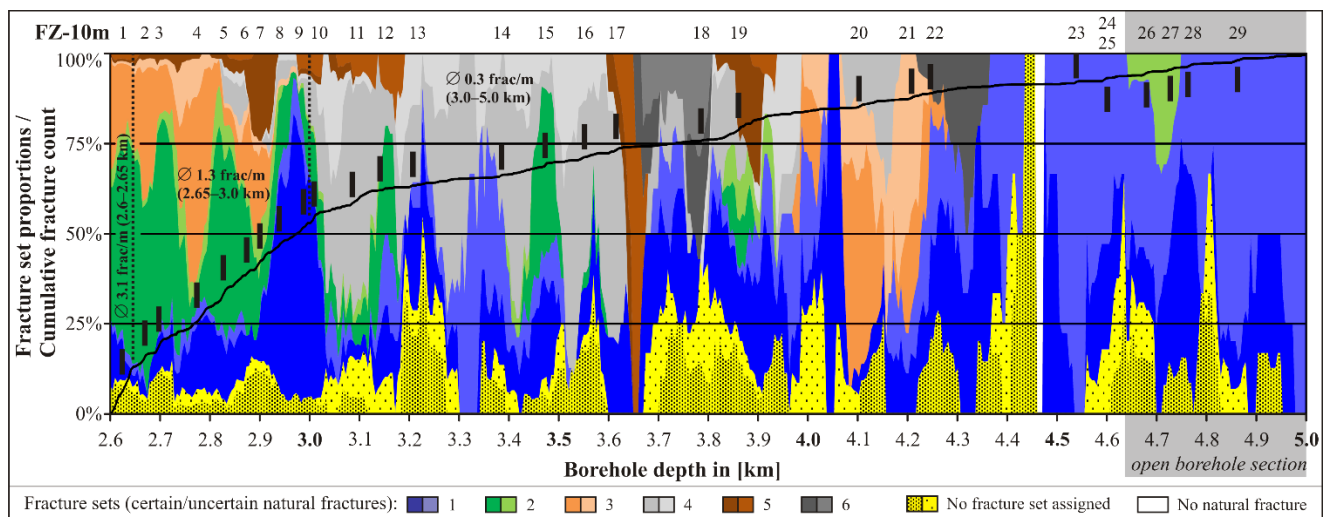


**Figure 1** Relative distribution of the six sets of fractures identified in the analysis of the natural fractures. The solid line denotes the cumulative number of all types of fracture identified.

The second component is to evaluate the linkage between the distributions of fracture length, stress variations and induced seismicity. The objective is to assess whether the observable scaling of stress variations and seismic magnitude can be used to constrain the scaling of fracture length, a parameter that is difficult to estimate from borehole observations alone. In a paper presented at the Discrete Fracture Network Engineering conference in 2014, we assessed the practicality of using the pattern of stress variability around natural fractures to directly (i.e. deterministically) constrain the characteristics of the fractures that are otherwise not determinable, such as length. The assumption underpinning the analysis is that the observed stress variability along boreholes is solely a consequence of the perturbations associated with natural fractures. A sensitivity study on a single fracture embedded in perfectly-elastic media shows that the key parameters that influence the stress variability pattern are geometrical characteristics of the fracture, notably length, the intersection point of the borehole relative to the fracture tips, and the fracture dip. Mechanical characteristics like fracture strength and far field stress do not strongly influence the pattern of stress variability. The range of influence of a fracture scales linearly with the fracture length. For a single fracture, an inverse approach can be used to determine the geometrical characteristics of the fracture from the pattern of stress variation it produces along the hole. However,

for fracture networks, the stress variations along the hole arising from the interactions of the stress perturbations from multiple fractures that cut the borehole, as well as perturbations from fractures that are close to but do not intersect the well, become sufficiently complex that inversion for geometrical characteristics of the fractures is not practicable. In this case, a statistical approach that relates the wavelength distribution of the stress variability to the distribution of fracture length could be more successful. Future work will examine this.

### **1.1.3 Assessment of thermal stimulation data and procedures used in Iceland (Task 1.3a)**

Geothermal wells are usually stimulated following drilling in order to improve their connectivity with the reservoir. In the case of Enhanced Geothermal Systems, high-pressure injections are used to create the reservoir itself (hydraulic stimulation). Chemical treatments with acid are commonly used for wells accessing sedimentary geothermal reservoirs. In Iceland, where most reservoirs are in volcanic rocks and at high temperature, cold-water injections at modest pressures are used to improve the connection with the reservoir, as measured by an increase in the injectivity of the well. The process is referred to as thermal stimulation, since it is believed to involve mechanisms that are activated by the cooling of the hot rock, with a limited contribution from hydraulic effects. In the case of wells in Iceland, the cleaning of drill cuttings from feed zones can also contribute to an improvement of injectivity, at least at early times in the stimulation process. Injectivity increases occurring at longer times are more likely to reflect the thermo-elastic response of the rock to cooling, which results in a progressive reduction in the effective normal stress acting on feed zones that take the flow. This can lead either to mode-1 opening of the fracture, which is a largely reversible process, or to the initiation of shear displacement on the fracture, which gives rise to irreversible increases in injectivity. Thermal stimulation effects can be manifest in any well where cold fluid is injected into a formation, such as in water-flooding wells in oil reservoirs, or the hydraulic stimulation of EGS reservoirs. Despite its increasingly-recognized importance, thermal stimulation is not well understood.

To contribute to a better understanding of thermal stimulation, a Master's project was initiated to conduct a detailed analysis of several case studies where thermal stimulation procedures were applied to wells in high-temperature fields in Iceland. The wells were subjected to cycles of cold-water injection and warming, the entire operation typically lasting for weeks. Injection rates may be up to 60 l/s and net volumes in the range  $10^4$  -  $10^5$  m<sup>3</sup>. Pressure increases during injections are usually in the range 10-20 bar, and so hydraulic stimulation effects are unlikely to be large. The evolution of well injectivity with cumulative injected volume during the operations was derived with a view to identifying the mechanisms underpinning the observed increases in injectivity. Relatively large, often erratic increases at early-time were taken to indicate cleaning of drill cuttings from feed-zones, whereas subsequent increases which tended to be smooth were interpreted as reflecting thermal effects. It was generally not possible to identify whether the increases were due to mode-1 opening or shear initiation because of the absence of sufficient experimental control, such as a repeat injection after the well had been allowed to fully recover to determine whether the improvements persisted. It was also impossible to distinguish between shearing and cleaning of drill cuttings, both of which are expected to produce irreversible increases in injectivity. This task is concluded.

### **1.1.4 Modeling of the thermal stimulation process (Task 1.3b)**

Work has progressed towards evaluating whether thermal effects could explain the onset of permeability enhancement at an unexpectedly low pressure of the principal feed zone in well BS-1 during the hydraulic stimulation of the Basel EGS reservoir. Since the focus is on near-well stimulation, where the flow-field is divergent, the model must necessarily be 3-D in nature. An initial attempt was made to build an elementary 3-D thermo-hydro-mechanically-coupled numerical model of the dominant feed-zone fracture identified in the Basel reservoir using the 3-DEC code of Itasca. The work was conducted as part of a Master's study (Hédinsdóttir, 2014), but the task could not be completed within the timeframe of the study period. Nevertheless, the work conducted identified basic numerical limitations in using 3-DEC for

coupled H-T-M problems. The work is being continued using a different code that is better suited to the problem.

## **Deliverables**

### – Task 1.2a

Valley, B., and K. F. Evans (2015). Estimation of the stress magnitudes in Basel Enhanced Geothermal System, paper presented at World Geothermal Conference 2015, International Geothermal Association, Melbourne, Australia, 19-24 April.

Valley, B., and K. F. Evans (2014). Preliminary assessment of the scaling relationships of in-situ stress orientation variations indicated by wellbore failure data, paper presented at European Regional Symposium on Rock Engineering and Rock Mechanics: Structures in and on Rock Masses, EUROCK 2014, Int. Soc. Rock, Vigo, Spain, 27-29 May.

### – Task 1.2b

Ziegler, M., Valley, B., Evans, K.F. (2015). Characterisation of natural fractures and fracture zones of the Basel EGS reservoir inferred from geophysical logging of the Basel-1 well. Proceedings World Geothermal Congress. International Geothermal Association, Melbourne, Australia, 19-25 April.

Valley, B., R. Jalali, M. Ziegler, and K. F. Evans (2014). Constraining DFN characteristics for deep geothermal projects by considering the effects of fractures on stress variability, paper presented at International Conference on Discrete Fracture Network Engineering, Vancouver, Canada, 19 -22 October.

### – Task 1.3a/b

Hédinsdóttir, H. (2014). Mechanisms of injectivity enhancement in the thermal stimulation of geothermal wells, Master's thesis, ETH Zürich, Switzerland.

## 2. Induced seismicity: Monitoring, risk assessment and management (Module 2)

Prof. Dr. Stefan Wiemer (SED)

Dr. Guilhem Aurélie (SED), Dr. Pierre Dublanchet (SED), Dr. Dimitrios Karvounis (SED),  
Dr. Anne Obermann(SED), Dr. Toni Kraft(SED), Lukas Heiringer (SED), Eszter Király (SED)

### 2.1 Main scientific achievements and deliverables

The work of the Module addresses the challenges related to the monitoring and to the risk assessment of induced seismicity. Based on the improved understanding of geomechanical processes (Module 1) and using the advanced modelling tools of Module 4, the module works to develop a probabilistic framework for the assessment of seismic risk in all phases of future EGS projects. Developing such a framework requires the application of a variety of forecast models on a range of existing data, using standardized and community-accepted performance measures applied in pseudo-prospective (i.e. causal) tests. Moreover, the module covers tasks concerned with the better understanding of the process of permeability creation that is central to the EGS technology.

Task	Description	2013												2014												2015												2016			
		Ma	Ju	Ju	Au	Se	Oc	No	De	Ja	Fe	Ma	Ap	Ma	Ju	Ju	Au	Se	Oc	No	De	Ja	Fe	Ma	Ap	Ma	Ju	Ju	Au	Se	Oc	No	De	Ja	Fe	Ma	Ap				
2.1a	Database of injections													D2.1a																											
2.1b	Sensitivity of Mmax																									D2.1b															
2.2a	Monte Carlo style simulation of the reservoir response																																					D2.2a			
2.2b	Data-mining based on a range of sequences																									D2.2b															
2.3a	Velocity tomography applied to the Basel reservoir													D2.3a																											
2.3b	Noise tomography applied To the Basel reservoir																																					D2.3b			
2.4	Imaging using migration based techniques													D2.4																											
2.5	Spatio-temporal failure of microseismic structures													D2.5																											

#### Deliverables description

D2.1a Report: Database of injections  
 D2.1b Report: Sensitivity of Mmax  
 D2.2a Report: Monte Carlo style simulation of the reservoir response  
 D2.2b Report: Data-mining based on a range of sequences  
 D2.3a Report: Velocity tomography applied to the Basel reservoir  
 D2.3b Report: Noise tomography applied to the Basel reservoir  
 D2.4 Report: Imaging using migration based techniques  
 D2.5 Report: Analysis of microseismic structures in Basel

#### Status

Delayed  
 Month 24  
 Month 36  
 Delivered  
 Delayed  
 Month 36  
 Delayed  
 Delivered

#### 2.1.1 Database of injections (Task 2.1a)

A database of case-histories on injection-induced seismicity for Europe was conducted as a collaboration between the CCES/CEM-funded GEOTHERM-1 and CARMA projects. This effort is progressively expanded with additional case studies from beyond Europe also in cooperation with the project GEOSIM. The importance of case studies is that they allow the impact of site-specific parameters such as depth and proximity to faults to be assessed. The maximum observed earthquake for a specific tectonic setting and injection scenario offer important constraints for improving our understanding of Mmax.

A QuakeML based database called "InduCat" for induced seismicity and hydraulic stimulation data has been developed. The database can be accessed through various web services (there's a web page, a

fdsn service and a Matlab access tool) but they are only accessible from within ETH (due to legal reasons mostly).

### 2.1.2 Sensitivity of Mmax (Task 2.1b)

The hydromechanical code CFRAC (McClure, 20102) that includes fluid flow in a discrete fracture network and rate-and-state friction along the fractures was evaluated for its capabilities in finding possible limitation of the maximum possible magnitude that can occur during reservoir stimulation. It was found that depending on stress magnitude and fracture orientation different slip run-out regimes may occur. These preliminary modeling efforts illustrate that an essential ingredient for modeling induced seismicity is an appropriate description of frictional behavior. A paper on this topic has been published (Gischig et al., 2015).

The maximum magnitude expected for an earthquake rupturing a pre-existing fault is strongly controlled by the proportion of the fault surface deforming aseismically. This effect will be investigated further within the next months, using a new mechanical model (Dublanchet et al., 2013) based on laboratory derived rate-and-state friction laws, allowing to model both aseismic behaviour and seismic instabilities on a fault plane in response to fluid related stress perturbations.

In addition, in Mignon et al. (2015), the sensitivity to Mmax was considered as part of the probabilistic seismic hazard study for the Basel injection. This work now forms the baseline for the seismic hazard assessment, part of the environmental impact assessment, of the Bassecourt deep geothermal project on the canton Jura (proposed by GeoEnergie Suisse AG).

### 2.1.3 Monte Carlo style simulation of the reservoir response (Task 2.2a)

A new hybrid model has been developed and it is ready to be used for Monte Carlo simulations of the reservoir response. This hybrid model combines three-dimensional discrete fracture flow numerical

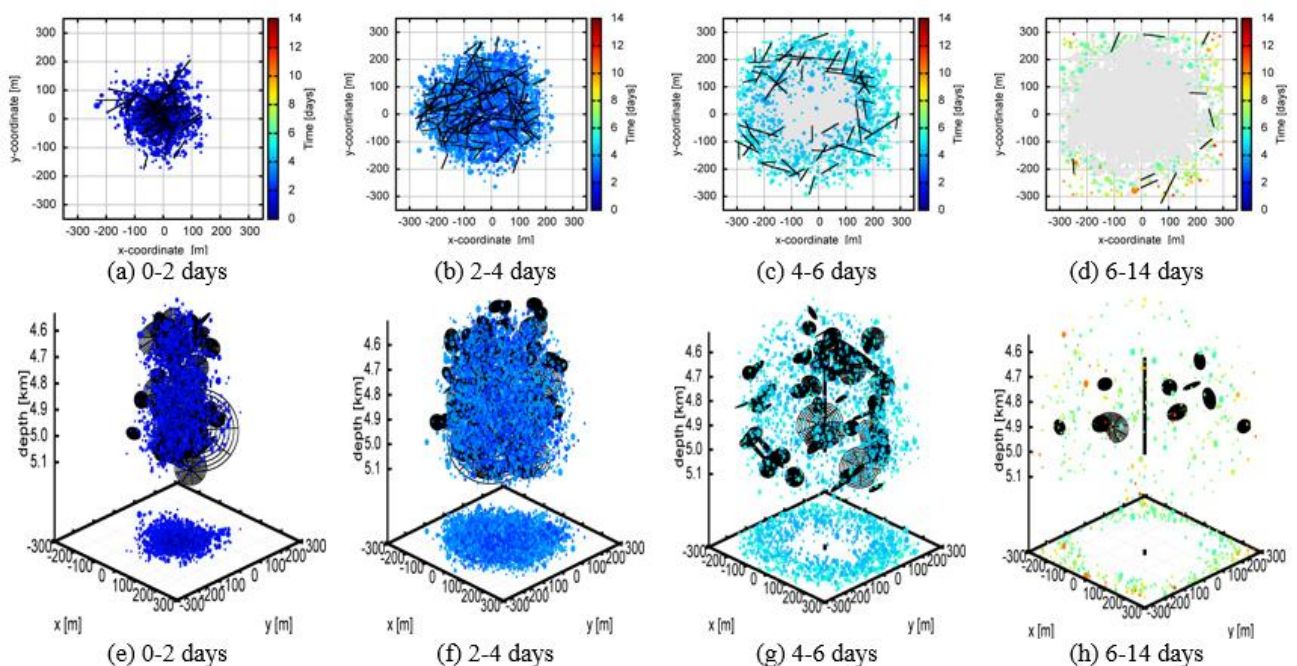


**Figure 2** The hybrid model is employed once for a 4-steps injection scenario. Injection increases by 10 l/s every 24 hours and the well shuts down on day 4. Figs. (a)-(d) are map views of the simulated seismicity, where the strike line of the large discrete fractures is plotted. Figs. (e)-(h) are three-dimensional plots with the position in space of all small earthquakes (colored dots) and the position in space of the large HFR-Sim fractures (black discs).

modelling with stochastic geo-mechanic considerations (the so-called 'seed model'). The EGS simulator 'HFR-Sim', which is a product of the project Geotherm-1, is used for modelling flow and heat transport inside EGS models. HFR-Sim provides fast and accurate solutions of the pressure field to the seed-model, which updates the catalogue of seismicity with new events and updates the discrete fracture network that is simulated by HFR-Sim, henceforth. The large earthquake events introduce new discrete fractures in the EGS model and the smaller ones affect the permeability of the damaged matrix (Figure 2). Monte Carlo simulations can be also performed with this hybrid model in order to assess the eventual thermal revenues of each studied scenario. Finally, the code for performing Monte Carlo simulations has been developed. Furthermore, it has been coupled with the hybrid model and it is currently optimized for the needs of the novel hybrid model. According to the initial timeline this task was supposed to start during the second year of the project, therefore Task 2.2a is one year ahead of the timetable.

**2.1.4 Data-mining based on a range of sequences (Task 2.2b)**

Within this task, we are developing a seismicity modelling test bench for Deep Geothermal Systems (Figure 3). The aim is to build and test existing and upcoming induced seismicity models in order to find key phenomena of induced seismicity hence develop precise and quick models. These models might be good candidates to build up an on-site decision making tool in Deep Geothermal Systems to plan the reservoir and control induced seismicity.

**INDUCED SEISMICITY MODELING TEST BENCH**

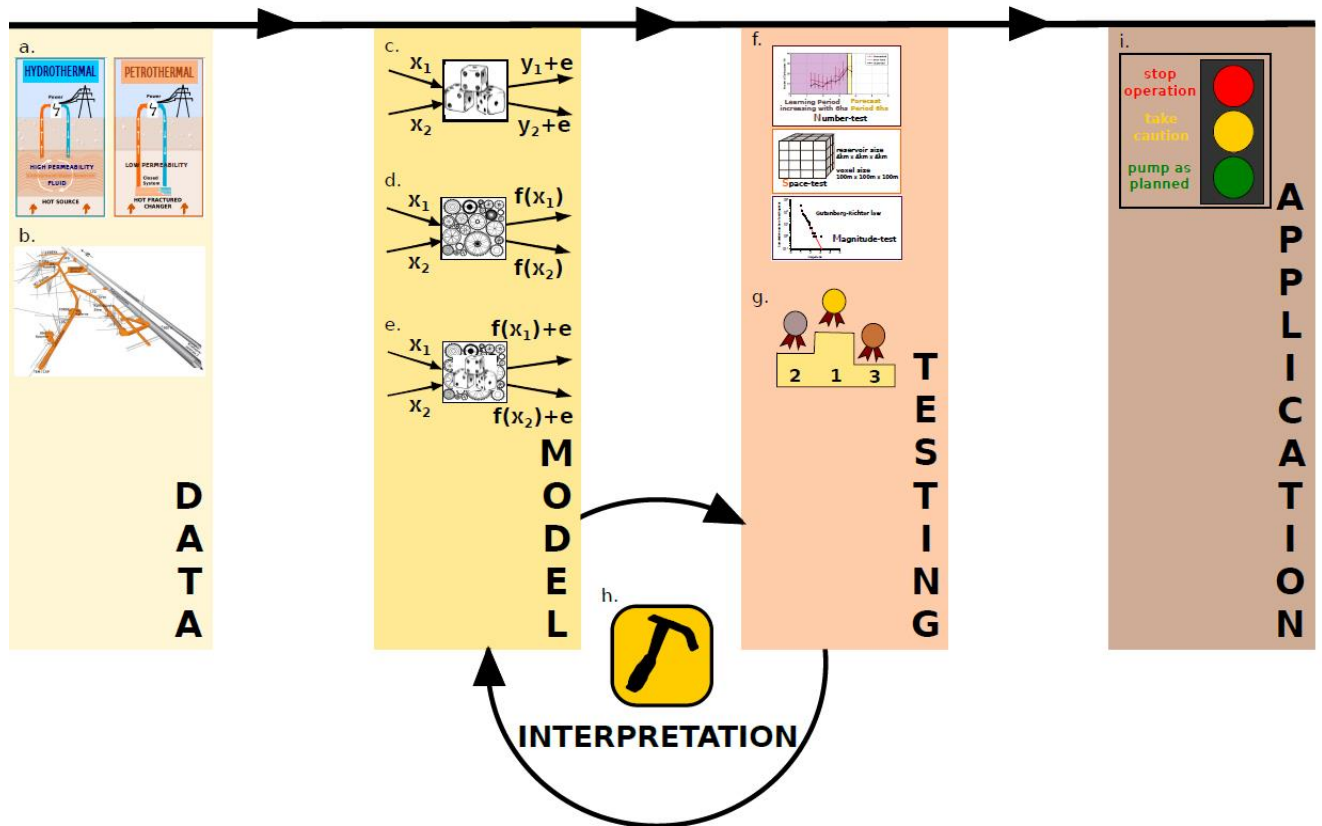


**Figure 3** Seismicity modelling test bench for Deep Geothermal Systems (from Kiraly et al.,2015)

As a first step, we consider the Basel 2006 dataset and generate forecasts of the number and spatial distribution of seismicity in the next six hours. We explore two models: (1) a hydro-geomechanical stochastic seed model based on pore pressure diffusion with irreversible permeability enhancement; and (2) four variants of a 3D "Shapiro" model which combine estimates of seismogenic index with a spatial forecast based on kernel-smoothed seismicity and temporal weighting. For both models, hydraulic and seismic parameters are calibrated against data from a learning period (starting at the beginning of injection) every six hours. We assess the models using metrics developed by the Collaboratory for the Study

of Earthquake Predictability (CSEP, [www.cseptesting.org](http://www.cseptesting.org)): we check the overall consistency of forecasts with the observations by comparing the number, magnitude and spatial distribution of forecast events with the observed induced earthquakes. We also compare the models with each other in terms of information gain, allowing pairwise ranking.

In the near future, we intend to involve other models (e.g. fully-coupled HFR-Sim) as well as other datasets, such as the injections at Soultz-sous-Forets, Rosemanowes, Gross Schoenebeck, Iceland, Australia in the testing framework. The work of this task is slightly delayed due to difficulties in retrieving the necessary data sets from some of the sites mentioned above.

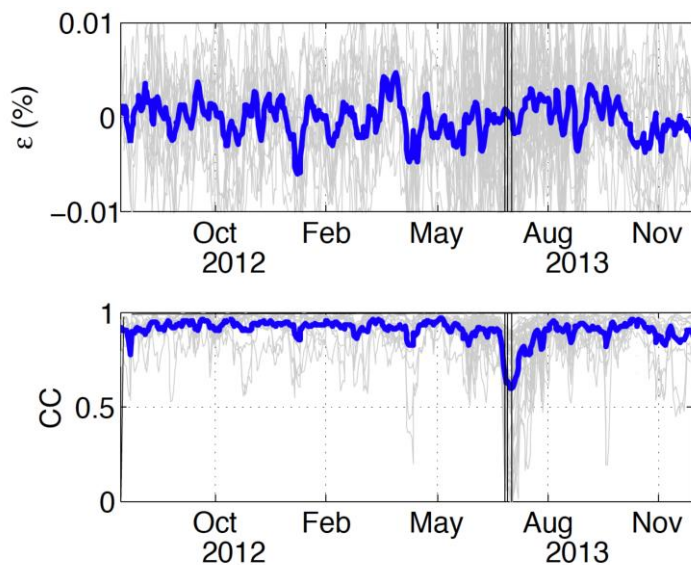
### 2.1.5 Velocity tomography applied to the Basel reservoir (Task 2.3a)

This task will only start later in the project.

### 2.1.6 Noise tomography applied To the Basel reservoir (Task 2.3b)

We applied noise interferometry techniques to the continuous data sets from the Basel and St. Gallen geothermal experiments. The application of passive methods allows in the case of Basel (Hillers et al. 2015) the detection of an aseismic transient of  $\sim 35$  days duration that begins with the onset of the reservoir stimulation; and in the case of St. Gallen (Obermann et al. 2015) the detection of a perturbation of the seismic waveform that is related to aseismic changes in the medium properties associated with the reservoir stimulation.

We show with those applications that noise interferometry can provide critical observables that are complementary to results obtained with standard microseismicity tools. Passive monitoring and imaging has the potential to mature into routinely applied observation techniques that support reservoir management in a variety of geotechnical contexts such as mining, fluid injection, fracking, nuclear waste management, and CO<sub>2</sub> storage.



complementary to results obtained with standard microseismicity tools. Passive monitoring and imaging has the potential to mature into routinely applied observation techniques that support reservoir management in a variety of geotechnical contexts such as mining, fluid injection, fracking, nuclear waste management, and CO<sub>2</sub> storage.

**Figure 4:** a) Apparent velocity changes; b) waveform coherence CC. The thick blue lines are the averages over all station pairs  $ij$ . The vertical lines mark the injection tests and the ML3.5 earthquake (from Obermann et al., 2014)

### 2.1.7 Imaging using migration based techniques (Task 2.4)

This task will only start later in the project

### 2.1.8 Spatio-temporal failure of microseismic structures (Task 2.5)

The work of this task has been concluded and the results are presented in the papers of Deichmann et al (2014) and Kraft et al. (2014) on Geothermics. In addition, as part of this task, we are investigating the spatio-temporal evolution of the seismicity in St. Gallen. Diehl et al. (2014a, 2014b) performed a high-precision relative relocation of the seismicity. Kraft et al. then used this work as an input for a preliminary analysis of the time line of the seismicity evolution. Finally, Edwards et al., (2014) investigated the ground motions and stress drops of the events in Basel and St. Gallen.

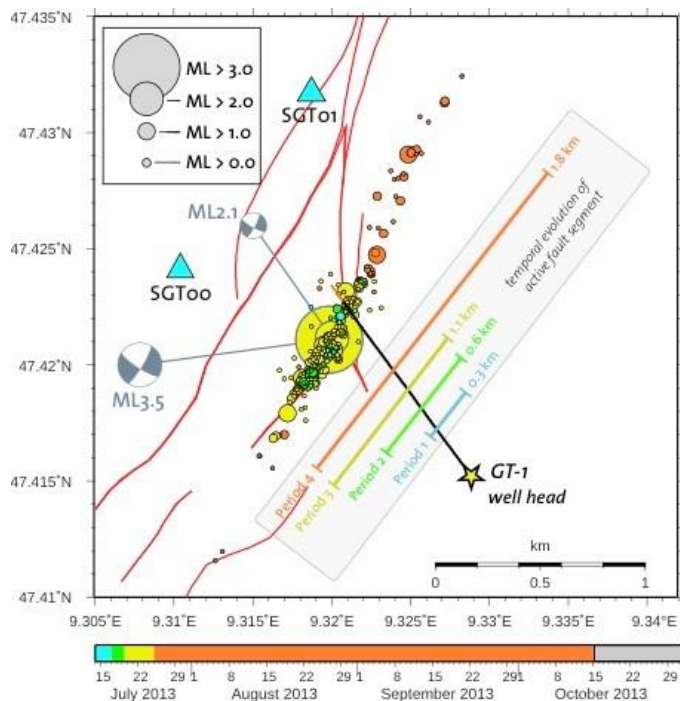


**Figure 5** Localization of hypocenters in St. Gallen

## Deliverables

### – Task 2.1b

Dublanchet P., Bernard P., Favreau P. (2013). Creep modulation of Omori law generated by a Coulomb stress perturbation in a 3-D rate-and-state asperity model, *Journal of Geophysical research*, 118, 9, 4774-4793.

Gischiga, V. S., Eberhardta, E., Mooreb, J., R., Hungra O., (2015). On the seismic response of deep-seated rock slope instabilities – Insights from numerical modelling, *Engineering Geology*, 193, 1–18.

### – Task 2.2a

Karvounis D., Wiemer S. (2015). Decision Making Software for Forecasting Induced Seismicity and Thermal Energy Revenues in Enhanced Geothermal Systems, *Proceedings World Geothermal Congress 2015* (accepted), Melbourne, Australia, 19-25 April 2015.

Karvounis D., Gischig V., Wiemer S. (2014). Towards a Real-Time Forecast of Induced Seismicity for Enhanced Geothermal Systems, *ASCE, Shale Energy Engineering Conference*, Pittsburgh 21-23 July 2014.

Karvounis D., Gischig V., Wiemer S. (2014). EGS Probabilistic Seismic Hazard Assessment with 3-D Discrete Fracture Modeling, *Stanford Geothermal Workshop*, Stanford, USA, 24-26 February 2014.

### – Task 2.2b

Király E., Gischig V., Karvounis D.C., Wiemer S. (2014) Validating Models to Forecasting Induced Seismicity Related to Deep Geothermal Energy Projects. *PROCEEDINGS, Thirty-Ninth Workshop on Geothermal Reservoir Engineering* Stanford University, Stanford, California, February 24-26, 2014

online: <https://pangea.stanford.edu/ERE/pdf/IGStandard/SGW/2014/Kiraly.pdf>



Király E., Gischig V., Karvounis D.C., Heiniger L., Wiemer S. (2014). Forecasting Induced Seismicity In Deep Geothermal Energy Projects. Geophysical Research Abstracts Vol. 16, EGU2014-12511, EGU General Assembly April 27-May 02, 2014

online: <http://meetingorganizer.copernicus.org/EGU2014/EGU2014-12511.pdf>

Király E., Zechar J D., Gischig V., Karvounis D., Heiniger L., Wiemer S. (2015) Modeling and Forecasting Induced Seismicity In Deep Geothermal Energy Projects. Submitted to Proceedings World Geothermal Congress 2015. Melbourne, Australia, 19-25 April 2015

– Task 2.3b

Hillers G., Husen S., Obermann A., Planès T., Larose E., (2015). Noise based monitoring and imaging of aseismic transient deformation induced by the 2006 Basel reservoir stimulation. Geophysics doi: 10.1190/GEO2014-0455.1.

Obermann A., Kraft T., Larose E., Wiemer S. (2015). Potential of ambient seismic noise techniques to monitor reservoir dynamics at the St. Gallen geothermal site. JGR, doi: 10.1002/2014JB011817.

Obermann A., Larose E., Wiemer S. (2014). Potential of ambient noise techniques to monitor reservoir dynamics at the St. Gallen geothermal site, AGU conference, San Francisco, USA, 15-19 December 2014.

– Task 2.5

Deichmann N., Kraft T., Evans K. (2014). Identification of faults activated during the stimulation of the Basel geothermal project from cluster analysis and focal mechanisms of the larger magnitude events, *Geothermics*, 52, 84-97.

Diehl, T., J. Clinton, T. Kraft, S. Husen, K. Plenkers, A. Guilhelm, Y. Behr, C. Cauzzi, P. Kästli, F. Haslinger, D. Fäh C. Michel and S. Wiemer (2014). Earthquakes in Switzerland and surrounding regions during 2013, *Swiss Journal of Geosciences*, October 2014; DOI: 10.1007/s00015-014-0171-y

Diehl, T., Kraft, T., Kissling E., Deichmann N., Clinton, J., and Wiemer, S. (2014b). High-precision relocation of induced seismicity in the geothermal system below St. Gallen (Switzerland). Poster Presentation, EGU Annual Meeting, Vienna, Austria.

Edwards, B. and J. Douglas (2014). Magnitude Scaling of Induced Earthquakes. *Geothermics*, doi: 10.1016/j.geothermics.2013.09.012.

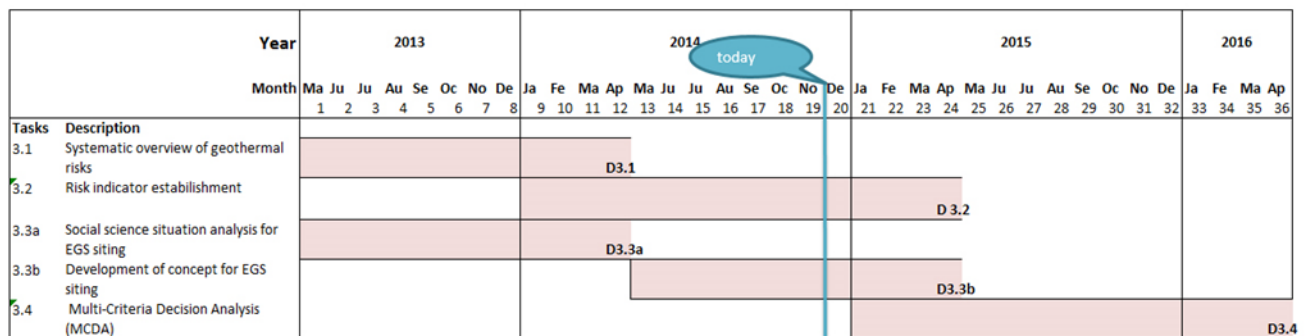
Kraft T., Deichmann N. (2014). High precision relocation and focal mechanism of the injection induces seismicity at the Basel EGS, *Geothermics*, 52, 59-73.

### 3. Comparative assessment of accidental risks and social acceptance (Module 3)

Dr. Peter Burgherr (*Laboratory for Energy systems Analysis, Technology Assessment group, PSI-TA*)  
 Dr. Matteo Spada (*PSI-TA*), Dr. Emilie Sutra (*PSI-TA*)  
 Dr. Michael Stauffacher (*Institute for Environmental Decisions ETH-USYS*),  
 Dr. Corinne Moser (*ETH-USYS*), Nora Muggli (*ETH-USYS*),

#### 3.1 Main scientific achievements and deliverables

Module 3 comprises four distinct tasks. PSI’s Technology Assessment (TA) group focuses on comparative risk assessment (tasks 3.1, 3.2) and the development of a Multi-Criteria Decision Analysis (MCDA) framework (task 3.4), whereas the Institute for Environmental Decisions (IED) at ETHZ establishes a concept for public and stakeholder involvement in the siting of pilot projects (task 3.3).



**Deliverables description**

- D3.1 Report: overview of geothermal risks [based on extensive literature survey]
- D3.2 Report: Risk indicator report
- D3.3a Report: social science situation analysis for EGS siting
- D3.3b Report: development of concept for EGS siting
- D3.4 Report: outcome of Multi-Criteria Decision Analysis (MCDA)

**Status**

- Delivered
- Month 24
- Delivered
- Month 24
- Month 36

#### 3.1.1 Systematic overview of geothermal risks (Task 3.1)

(Contributor: PSI-TA)

This task was carried out during the first project year that ended in April 2014. It aimed to provide a systematic overview of the various geothermal accident risks, focusing on human health effects and environmental impacts. It has been completed as scheduled, and the corresponding deliverable is available in the form of summary report. This work has also been presented at two conferences, i.e., SRA-Europe 2014 in Istanbul, Turkey (Sutra et al., 2014), and ESREL 2014 in Wroclaw, Poland (Spada et al., 2014). Furthermore, the research was closely coordinated with risk assessment activities in the TA Swiss project (Hirschberg et al., 2014). However, it should be noted that the relevant literature would be continuously screened and reviewed during the project duration to ensure that newly published information can be taken into account.

In task 3.1 a systematic literature review was carried out to identify specific risk factors that can potentially lead to accidental events. Table 1 provides an overview of the various accident risks associated with deep geothermal systems. It is important to note that in comparative risk assessment a full-chain approach (e.g., Burgherr & Hirschberg, 2014) is commonly applied because accidents can occur at all stages of an energy chain. In the context of geothermal systems this means that the drilling, the stimulation and the operational phases need to be taken into account.

Among the different risk aspects presented in Table 1, blowout accidents and the use of hazardous substances in the drilling (mud) as well as stimulation and operational (working fluids) phases are specifically assessed. Since deep geothermal systems have not yet been installed at many sites, historical ex-

perience in terms of accidents is rather limited, particularly if one compares it for example to fossil energy chains.

Therefore, the estimation of risk indicators for blowouts and hazardous substances is based on historical experience that can be considered a meaningful proxy for deep geothermal systems.

In all cases, accident data from OECD countries were used because they can be considered sufficiently representative for Switzerland in terms of safety standards and regulatory frameworks, whereas this cannot be assumed for non-member countries. However, in the case of hazardous substances it is necessary to focus on those chemicals that could be possibly used in Switzerland.

**Table 1:** Issues and risks related to a particular phase in Deep Geothermal Systems

Phase	Issue	Risk
Drilling	Drilling Muds	Risk related to the use of hazardous substances
Stimulation	Stimulation	Risk related to the use of hazardous substances
Drilling and Operational	Blowout	Risk related to blowout accidents
	Landslides	Risk related to landslide hazard
	Induced Seismicity	Risk related to induced seismicity hazard
Operational	Geofluids	Risk related to the hazardous substances brought to the surface by the circulation of the geofluids
	Cooling System	Risk related to the use of hazardous substances
	Working Fluids	Risk related to the use of hazardous substances

Historical accident data are collected from different primary information sources, such as FACTS (<http://factsonline.nl>), ARIA (<http://www.aria.developpement-durable.gouv.fr>), and the PSI's Energy-related Severe Accident Database (ENSAD). While the former two were used to analyze accidents caused by hazardous chemicals and blowouts, the database ENSAD was only used for blowout accidents. Caustic soda is commonly used as additive in the drilling mud, whereas benzene and toluene are possibly used as working fluids. In the former case, accidents related to transportation, storage and use in well drilling are considered. Concerning working fluids, the aforementioned cases for caustic soda as well as accidents attributable to the use of these chemicals in the geothermal power plant (e.g., due to leakage from a pipe or due to a valve failure) need to be taken into account.

Due to the lack of blowout accident data for geothermal systems, onshore accidents in the natural gas energy chain were considered a first order approximation for geothermal drilling because it generally relies on the same kind of technology used in the oil and natural gas (O&G) industry, modified for high temperature applications and larger well diameters (e.g., Finger & Blankenship, 2010).

To ensure a fair, transparent and consistent comparison of risk indicators, they should be expressed in a common format, i.e. that they are normalized to the same reference unit. In order to ensure straightforward comparisons with previous PSI studies, the risk indicators for both blowout and hazardous substances are normalized to the unit of Giga-Watt electric year (GWeyr). Furthermore, risk indicators are calculated for three distinct cases, namely a base, high capacity and low capacity case as defined in the TA-Swiss study (Treyer et al., 2014). In this way risk assessment and Life Cycle Assessment (LCA) results are based on the same set of assumptions, (see Table 2 modified from Treyer et al., 2014).

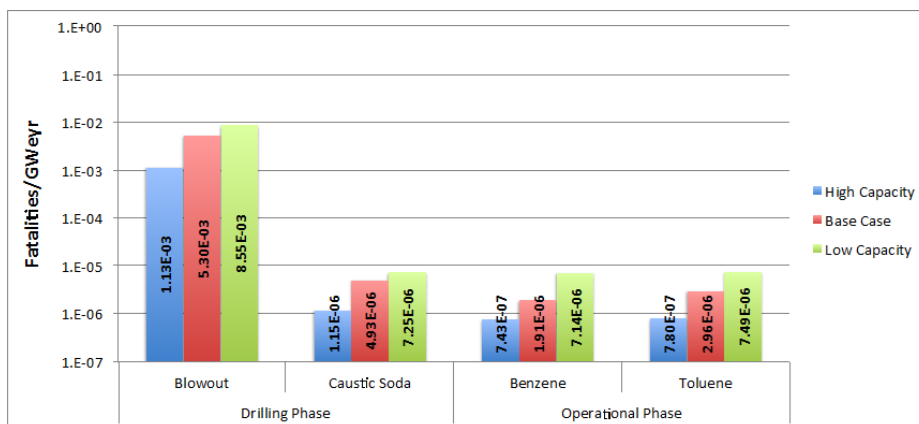
**Table 2:** Key parameters for the different deep geothermal power plants used in this study

	Medium capacity (Base case)	High capacity	Low capacity
Net plant power	5.5 MW <sub>e</sub>	14.6 MW <sub>e</sub>	2.9 MW <sub>e</sub>
Well depth	5 km	6 km	5 km
Number of wells	6 (2 well triplets during total lifetime)	3 (1 well triplet during total lifetime)	3 (1 well triplet during total lifetime)
Surface plant life time	30 yrs	30 yrs	20 yrs
Heat and power cogeneration unit, organic Rankine cycle, 1MW <sub>e</sub>	5.05	5.05	5.05
Caustic Soda as additive in the drilling mud	1 kg/m	1 kg/m	1 kg/m
Working Fluids used at the power plant at year 1	Benzene: 436 kg Toluene: 432 kg	Benzene: 436 kg Toluene: 432 kg	Benzene: 436 kg Toluene: 432 kg
Yearly losses of the working fluids	8%	8%	8%

For example, considering the base case shown in **Error! Reference source not found.**, as a first approximation, the use of caustic soda is considered constant for the entire drilling phase. Therefore, by considering a drilling depth of 5000 m and 6 wells over the plant lifetime of 30 years, the total amount of caustic soda used in the geothermal drilling phase equals 30,000 kg. In this case, it is assumed that the power plant of 5.5 MW<sub>e</sub> is able to generate 1.49E+9 kWh, which amounts to 1.70E-1 GWeyr over its entire lifetime. Therefore, the normalization factor is estimated as follows:

$$\begin{aligned}
 \text{Normalization Factor} &= \frac{\text{kg of substance used in the power plant}}{\text{total kg of substance product in the time period 1990 – 2012}} \\
 &= \frac{1}{1} \cdot \frac{\text{kg of substance used in the power plant}}{\text{GWeyr product in the power plant over its lifetime}}
 \end{aligned}$$

The total production of caustic soda in OECD countries in the time period 1990-2012 amounts to 1.07E+12 kg. Therefore, the normalization factor for the risk indicator would be 1.64E-7 1/GWeyr. The same approach is applicable to the working fluids, considering that, additionally, the yearly losses over the entire lifetime need to be accounted for. For blowout accidents, in the equation above the use of substance in kg at the power plant needs to be replaced by the



number of drilled wells over the lifetime, and the total production with the total number of drilled wells in the time period of interest.

**Figure 5** Fatality rate for onshore blowouts and the three hazardous substances analyzed, based on accident data from OECD countries (1990-2012), and for three different geothermal power plant cases.

Figure 5 shows normalized fatality rates (fatalities/GWeyr) for all three analyzed cases. Overall, blowout risk is about three orders of magnitude higher than for hazardous substances used in both the drilling and operational phases.

In the remaining time of Task 3.2, substances used during stimulation, such as hydrogen chloride (HCl) and hydrofluoric acid (HF), will be analyzed.

### 3.1.2 Risk indicator establishment (Task 3.2)

*(Contributor: PSI-TA)*

The task has started in the last quarter of project year 1, and should be completed by the end of project year 2. The main goal is to establish a set of risk indicators for geothermal energy systems. While PSI's TA group addresses accidental risks, other tasks (e.g. 3.3) and modules (e.g. 2 and 6) should complement the final indicator set. The latter is then evaluated by means of Multi-Criteria Decision Analysis (MCDA) (task 3.4). The assessment of accident risks considers hazardous substances used during drilling, stimulation and operation of a deep geothermal system, as well as blowouts. In a first step, different types of consequence indicators have been quantified for human health effects (e.g., fatalities, injuries and evacuees), and environmental impacts (e.g., release of a substance). In a second step, a preliminary exposure and toxicity assessment is planned, which allows comparing effects of different chemicals on human health and the environment (e.g., Meiners et al., 2013). The Hazardous Quotient (HQ) provides a useful starting point to determine the risk level of a given chemical used in geothermal energy systems. This information can then help to compare different chemicals and different, previously defined, test cases.

Finally, in January 2015 Task 3.4 will start, which aims to develop a MCDA framework.

### 3.1.3 Concept for public and stakeholder involvement (Task 3.3)

*(Contributor: ETH-IED)*

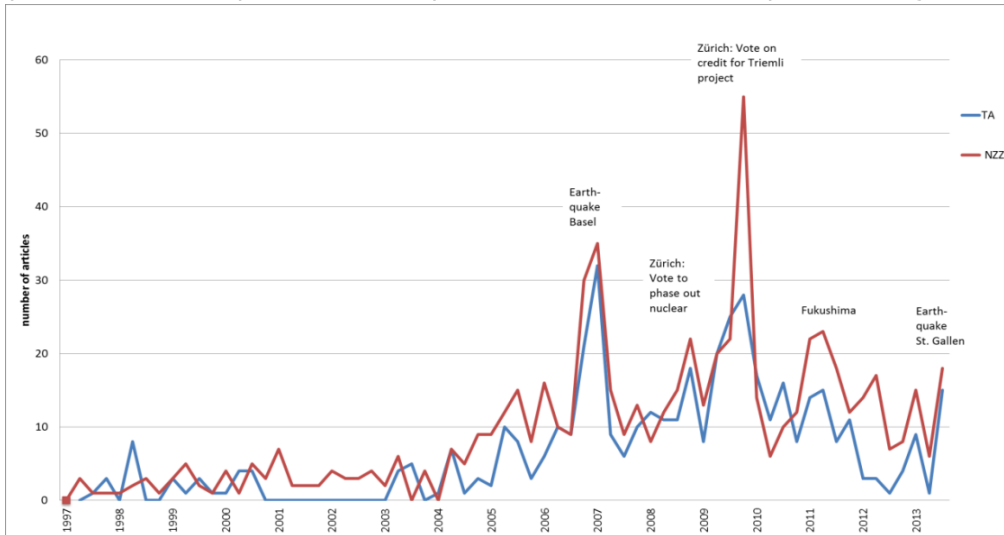
Within Task 3.3, the project is progressing well. A detailed social science situation analysis for EGS siting was performed during 2013 and finalized in 2014. Major work during 2014 was the revision process for two book chapters (as part of the TA Swiss project) and the writing of a research paper on the media analysis.

In addition, the project of St. Gallen was reviewed based on written documentation and first contacts established with responsible stakeholders (inter alia a first personal exchange with Stadtrat Fredy Brunner took place). Preparation for a teaching course called Transdisciplinary Case Study (tdCS) is underway. Students will retrospectively analyze the project of St. Gallen especially focusing on public and stakeholder involvement. It seems essential to profit as much as possible from experiences in St. Gallen for future projects. Although the project was stopped it can certainly be used as best-practice at the level of communication and public involvement. Yet relevant evidence needs to be systematically collected and analyzed. At the moment we are restricted to unstructured and non-systematic oral information only<sup>1</sup>. The tdCS is a course of the Masters program in Environmental Sciences - Major in Human-Environment Systems (7 CP), suitable for other Masters as well. It is a course offering specific learning opportunities in line with ideas from project-oriented and problem-based learning. Students work in groups, get a high level of autonomy, and work in a methodologically sound manner and together with stakeholders from practice. tdCS are embedded in on-going research projects, focus on real-world problems and thus allow for a genuine and challenging research and learning environment. In 2015, Stefan Wiemer and Michael Stauffacher will lead the tdCS.

---

<sup>1</sup> See e.g. the following video <http://www.geothermie.stadt.sg.ch/aktuell/details-video/artikel/3-geothermie-kongress-stgallen-rueckblick.html>

With respect to main scientific achievements, two core elements were combined: a review of scientific literature and a media analysis. A broad review of scientific literature focusing on existing studies on the perception of deep geothermal and other contested energy technologies (nuclear waste, wind power and CCS) provided essential information on the scientific state-of-art in the field. A thorough analysis of all media articles between 1997 and 2013 in the Neue Zürcher Zeitung (NZZ) and the Tages-Anzeiger (TA) allowed insights into the ways how deep geothermal energy is presented in the media and which arguments are used by whom. Overall, our work points to public perception that is probably still highly volatile, with many people holding ambivalent opinions. More knowledge is necessary to understand the present state of opinion and the potential mechanisms of opinion change. Events involving planned future projects and their media coverage will certainly play a considerable role in affecting and fixing public opinion. Thus, attention should be placed on these non-technical aspects of deep geothermal energy.



future projects and their media coverage will certainly play a considerable role in affecting and fixing public opinion. Thus, attention should be placed on these non-technical aspects of deep geothermal energy.

**Figure 6** Frequency of newspaper articles containing the keywords "Geothermie or Erdwärme" over time in TA and NZZ (N = 1119 articles).

**Table 3** Distribution of arguments of the different actor groups within the identified frames (N = 382 arguments attributable to specific actor groups).

	Energy transition		Risks		Technology		Costs		Total
	Opportunity (n=90)	Unrealistic option (n=12)	Uncertainties and risks (n=71)	Risks under control (n=66)	Benefits (n=33)	Handicaps (n=43)	Economic (n=14)	Expensive (n=53)	
Politicians (n=128)	21%	8%	9%	16%	9%	15%	3%	18%	100%
Public authorities (n=67)	25%	0%	19%	18%	4%	13%	1%	18%	100%
Industry (n=99)	40%	0%	6%	15%	13%	6%	8%	11%	100%
Scientists (n=88)	7%	2%	45%	20%	6%	10%	1%	8%	100%

In 2015 the following major project steps are planned:

- From February until June 2015 a Transdisciplinary Case Study on the geothermal project in St. Gallen will be organised (teaching course of 7 CP in the Masters programme in Environmental Sciences - Major in Human-Environment Systems). Students will retrospectively analyse the project of St. Gallen especially focussing on public and stakeholder involvement.
- Further, a Master thesis should start in March 2015 focussing on the communication of uncertainties. Research literature from other issues will be reviewed (like for instance climate change and

health prevention) and concrete experimental work developed (e.g. confronting selected people with varying presentations of uncertainties).

- Finally, conceptual work will start addressing the following core questions in public and stakeholder involvement: Why should the public or stakeholders be involved? Who should be involved and who does the involving? When should the public at large and other stakeholders be involved? On which specific issues should the participants be involved and what is their expected contribution? Which method allows for appropriate participation?

## Deliverables

- Task 3.1

Spada, M. & Burgherr, P. (2014) 'Accident Risks' in Hirschberg, S., Wiemer, S & Burgherr, P. (eds.): *Energy from the earth: Deep geothermal as a resource for the future?*, TA-Swiss, Bern, Switzerland, pp. 220-251

Sutra, E., Spada, M., Wolf, S., & Burgherr, P., (2014). Comparative Risk Assessment for Hydraulic Fracturing in Shale Gas and Deep Geothermal Systems. 23<sup>rd</sup> SRA-Europe conference, Istanbul, Turkey, June 16-18.

Spada, M., Sutra, E., Wolf, S. & Burgherr, P. (2014). Accident Risk Assessment for Deep Geothermal Energy Systems. Proceedings for the European Safety and Reliability Conference, ESREL 2014, 14-18 September 2014, Wroclaw (Poland). In: *Safety and Reliability: Methodology and Applications* (Nowakowski T., Mlynczak M., Jodejko-Pietruczuk A., Werbinska-Wojciechowska S. (Eds.)).

- Task 3.3a

Within Task 3.3, two chapters for a book publication were produced, one on the literature review and the other on the content analysis of newspaper articles. The latter was presented at an international conference and prepared as scientific article for an international journal (submitted in Summer 2014). Main products are as follows:

Moser, C., & Stauffacher, M. (2015). Literature review: Public perception of geothermal energy. In S. Hirschberg, S. Wiemer & P. Burgherr (Eds.), *Energy from the earth: Deep geothermal as a resource for the future?* TA-SWISS 62/2015. Zürich: vdf Hochschulverlag (pp 297-306)

Muggli, N., Moser, C., & Stauffacher, M. (2015). Content analysis: media articles on deep geothermal energy in Switzerland. In S. Hirschberg, S. Wiemer & P. Burgherr (Eds.), *Energy from the earth: Deep geothermal as a resource for the future?* TA-SWISS 62/2015. Zürich: vdf Hochschulverlag (pp 306-27)

Stauffacher, M., Muggli, N., Scolobig, A. & Moser, C. (2014, submitted for publication). Framing deep geothermal energy in mass media: the case of Switzerland. *Technological Forecasting and Social Change*.

## References

Burgherr, P. & Hirschberg, S. (2014). Comparative Risk Assessment of Severe Accidents in the Energy Sector, *Energy Policy*, doi: 10.1016/j.enpol.2014.01.035

Finger, J. & Blankenship, D. (2010). *Handbook of Best Practices for Geothermal Drilling*. Sandia National Laboratory, Albuquerque, NM and Livermore, CA, USA, pp. 84.

Hirschberg, S., Wiemer, S & Burgherr, P. (eds.) (2014). *Energy from the earth: Deep geothermal as a resource for the future?* TA-Swiss, Bern, Switzerland.

Meiners, H. G., Denneborg, M., Müller, F., Bergmann, A., Weber, F.-A., Dopp, E., Hansen, C., Schüth, C., Gassner, H., Buchholz, G., Sass, I., Homuth, S. & Priebes, R. (2013). *Environmental Impacts of Fracking Related to Exploration and Exploitation of Unconventional Natural Gas Deposits*. Federal Environment Agency, Germany.

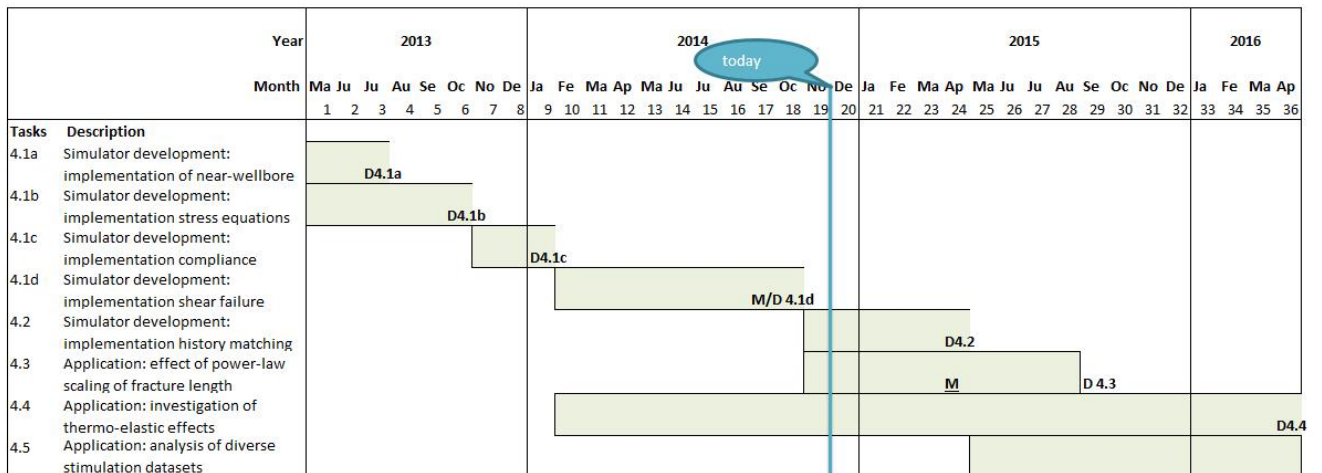
Treyer, K., Oshikawa, H., Bauer, C. & Miotti, M. (2014). 'WP4: Environment' in Hirschberg, S., Wiemer, S & Burgherr, P. (Eds.). *Energy from the earth: Deep geothermal as a resource for the future?* TA-Swiss, Bern, Switzerland, pp. 177-219.

## 4. A 3-dimensional H-T-M-coupled simulator for EGS reservoir creation and production (Module 4)

Prof. Dr. Patrik Jenny (*Department of Mechanical and Process Engineering, ETH-MAVT*)  
 Deb Rajdeep (*ETH-MAVT*)

### 4.1 Main scientific achievements and deliverables

Module 4 extends the hydro-thermally (H-T) coupled fractured reservoir simulator developed in GEOTHERM-1 with the implementation of stress and geomechanics in order to include the effects of fracture compliance and shear failure on the temperature and flow field. The main scientific achievement of this module is to develop an efficient numerical model to simulate the shear failure in fractured reservoir and, thus, to obtain the failure displacement along the fractures. A further investigation to improve efficiency and accuracy of this numerical method is ongoing. Furthermore, the coupling of this geomechanical failure model with the pressure field response in discrete fractures and rock matrix is part of the ongoing project.



**Deliverables description**

- D4.1a Implementation of near-wellbore non-Darcy flow with application to examples
- D4.1b Implementation of implementation stress equations
- D4.1c Implementation of implementation shear failure
- D4.1d Code developed together with documentation & report.
- D4.2 Report on history matching
- D4.3 Report (Joint with Task 1.1 of Module 1)
- D4.4 Report (Joint with Task 1.1 of Module 1)

**Status**

- Delivered
- Delivered
- Delivered
- Delayed
- Month 24
- Month 28
- Month 36

**Milestones description**

- M1 Completion of implementation of mechanics into reservoir simulator (Task 4.1d: required for simulation studies)
- M2 Completion of study of the implications of power-law scaling of fracture length

- Delayed
- Month 24

#### 4.1.1 Simulator development (Task 4.1)

The simulator development work can be subdivided into four project phases, which constitutes Task 4.1. Furthermore, in Task 4.2 a history-matching strategy to allow the simulator to be optimally used with data will be developed. The remaining tasks are related to the test of the simulator against the hypotheses developed in Modules 1 and 2 as well as on stimulation datasets of existing EGS.



#### 4.1.2 Simulator development: implementation of near-wellbore non-Darcy flow (Task 4.1a)

In EGSs, non-Darcy flow effects are usually strongest at the reservoir entry points where velocities in the fractures are high. Although such effects can have significant impact on the reservoir impedance, the capability to treat non-Darcy flow is rarely included in simulators, except as an approximation. Therefore, it is of great interest to accurately treat them in computational studies. A straightforward approach to include non-Darcy flow capabilities into an existing simulator is to implement the additional non-linear term in the Forchheimer equation, which requires iteration in order to compute pressure and flow solutions. Although this requires minor modifications of the existing code, it is more delicate to come up with an educated guess of the additional model coefficient. This can be implemented as parameter that can be adjusted to fit specific data sets. Once all coefficients are estimated, simulations of realistic scenarios will be conducted to investigate the importance of treating non-Darcy flow effects and to suggest improved operation strategies

#### 4.1.3 Simulator development: implementation of geomechanics into the simulator (Task 4.1b-d)

##### Failure Criteria and Slip Solution

Shear failure in a geomechanical domain can be achieved by a continuous increase in pore pressure via fluid injection in the fractures. This reduces the compressive force across the fracture plane and therefore the static friction limit of traction to compression ratio is reached. Given the normal unity vector to the fracture plane and the distribution of stress tensor field in the domain, the following equation defines the failure criteria at any point in the fracture plane:

$$\sigma_c = -\hat{n} \cdot \tilde{\sigma} \cdot \hat{n} \quad (1a)$$

$$\vec{\tau} = (\tilde{I} - \hat{n}\hat{n}) \cdot \tilde{\sigma} \cdot \hat{n} \quad (1b)$$

$$|\vec{\tau}| \leq (S_0 + \mu_s(\sigma_c - p)) \quad (1c)$$

The equation 1a defines the compressive force on a point in the failure plane, the equation 1b defines the traction force along the failure plane and the equation 1c defines the failure criteria for the fracture manifold. The term  $S_0$  defines a cohesive force on the fracture manifold. The effective normal traction force is obtained as a difference of total compressive normal force and the fluid pressure at a point along the fracture manifold. The term  $\mu_s$  defines an internal static friction coefficient. The slipping on the failure lines corresponds to a different timescale and this failure timescale is assumed to be much faster than the external boundary conditions and is of the order of wave propagation speed. This assumption couples the irreversible slip on the fracture plane with elastic displacements of the domain. Therefore, the timescale of slipping does not require being resolved in the numerical problem but rather a physical-relevant coupling of elastic displacements near the slipping plane with the slip is required.

##### Coupling with Fluid Solver

The typical fluid flow problem in a fractured reservoir involves flow along the discrete fractures and porous flow in the matrix. Darcy's law is governing such flow where the mass flux depends on the pressure gradient. The standard mass balance equation along a fracture and/or the matrix is given as

$$\frac{\partial E^i}{\partial t} - \nabla \cdot \left( \frac{b^i \mathbf{k}^i}{\mu} \cdot (\nabla p^i - \rho g) \right) + \Psi^{i \rightarrow d} = q^i, \quad (2)$$

$$\frac{\partial \phi^d}{\partial t} - \nabla \cdot \left( \frac{\mathbf{k}^d}{\mu} \cdot (\nabla p^d - \rho g) \right) + \Psi^{d \rightarrow i} = q^d \quad (3)$$

where equation 2 represents the flow along a single fracture involving mass transfer from neighbouring matrix and equation 3 represents the flow in the damaged matrix. The key variables of equation 2 are

pore volume per unit fracture area given as  $E^i$ , fracture aperture  $b^i$ , fracture permeability  $k^i$ , fluid viscosity  $\mu$ , fracture pressure  $p^i$ , the fracture to matrix mass transfer rate and the well injection rate  $q^i$ . The key variables of equation 3 are matrix porosity, matrix permeability  $k^d$ , matrix pressure  $p^d$ , the matrix to fracture mass transfer rate and the well injection rate  $q^d$ . The fracture pressure  $p^i$  has an important role also in the geomechanics of the problem. The pressure decreases the net compressive force being applied on the fracture due to external boundary conditions and thereby makes the fracture more prone to shear failure according to the equation 1c. The more injection of fluid eventually leads to shear failure. The result of the latter is a slip along the fracture planes. This increases the fracture aperture  $b^i$  and, eventually, permeability  $k^i$ . This slip also increases the fracture pore volume per unit fracture area  $E^i$ . The increase in aperture and pore volume due to fracture slip is rapid for small value of cumulative slip and slow for large value of cumulative slip. The dependence of aperture and pore volume is modelled here using two variables  $s_1$  and  $s_2$ . These two variables are described as follow:

$$s_1 = s \text{ (for } s < s_{max}), \quad (4)$$

$$s_1 = s_{max} \text{ (for } s \geq s_{max}), \quad (5)$$

$$s_2 = 0 \text{ (for } s < s_{max}), \quad (6)$$

$$s_2 = (s - s_{max}) \text{ (for } s \geq s_{max}), \quad (7)$$

where  $s_{max}$  is the maximum cumulative slip value up to which the hydraulic aperture and void aperture dependence is rapid. The equations describing the change in aperture is modelled as

$$b^i = b_0^i + \beta_1 s_1 + \beta_2 s_2, \quad (8)$$

where  $\beta_1$  is much larger than  $\beta_2$ . The dependence of void aperture of the fracture  $E^i$  on the slip and pressure is modelled as

$$E^i = E_0 + \left( \frac{a}{1 + (9\sigma'_n / \sigma_{nref})} \right) + \beta_1^* s_1 + \beta_2^* s_2. \quad (9)$$

The opening of the aperture provides more transmissibility of flow along the fracture. The change in void aperture creates a large volume to be filled. But the flow problem lags in filling up this newly created volume. That means the sharp change in geomechanics involve a small timescale in which the fluid flow problem cannot adjust to the newly created volume. Therefore, a relaxation model is needed which must involve a timescale over which this filling of pore volume takes place. Numerically also this kind of model provides a stability as otherwise sharp change in volume in very small time-step would involve a large source term for pressure change in the fracture, which may lead to numerical instability.

### Volume Relaxation Model

The modelling approach considered here is to update the change in void aperture in the equation 2 over a flow related timescale  $\tau^t$ . Thus, once a fracture unit fails, the flow problem along the fracture adjusts itself to the newly created void aperture given by the equation 9. Let  $E_f^i$  and  $E_*^i$  respectively denote fluid occupied void aperture and newly created void aperture after failure at a fracture unit. The change in this fluid volume aperture is modelled as

$$\frac{\partial E_f^i}{\partial t} = \frac{(E_*^i - E_f^i)}{\tau^t}. \quad (10)$$

This approach will allow the flow to couple with the sharp change in pore volume provided by the shear failure. Once the numerical timesteps resolve the timescale  $\tau^t$ , the problem of fluid occupied void aperture opening again become dependent on pressure.

### Results

Simulations being performed to study the effect of shear dilation failure in geomechanical domain due to fluid injection in fractures. The set up is a two dimensional square domain of extension 1KM×1KM in each of  $x$  and  $y$  direction. The constant shear and compressive force are applied in domain boundary and water is injected at the center of the fracture at a constant injection pressure/injection rate.

The mechanical properties for shear modulus and Poisson ratio are respectively 10 GPa and 0.1. The flow properties for fracture and damaged matrix are respective 0.1 mm for fracture aperture and  $10^{-13}$  m<sup>2</sup> for matrix permeability. The fracture is extended 500 meters from the center of the domain and oriented horizontally. The fracture has a constant static friction coefficient of 0.6 except for few nodes (located to the left of fracture center) where the static friction coefficient is 0.45. The propagation of the pressure signal from the fracture center to this weak zone leads to the first shear failure and the solution of flow field thereafter is depicted in Figure 7.

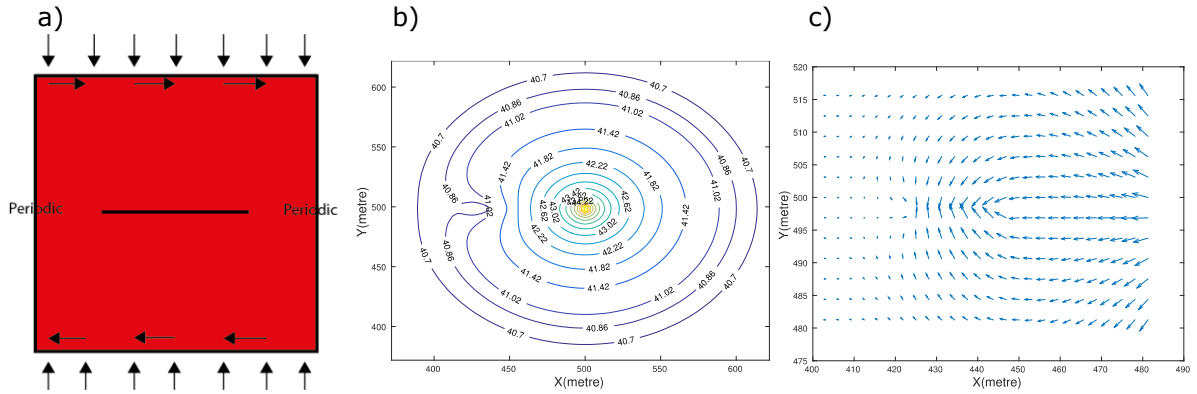


**Figure 7:** a) the problem setup; b) the pressure contour around the fracture just after failure; c) the flow of fluid from matrix to the fracture in the weak zone after the failure.

Another simulation with constant well injection rate of 1 m<sup>3</sup>/sec is performed to analyze the seismic events that occur for a duration of 10000 sec. The following figure shows the moment magnitude with time along due to water injection.

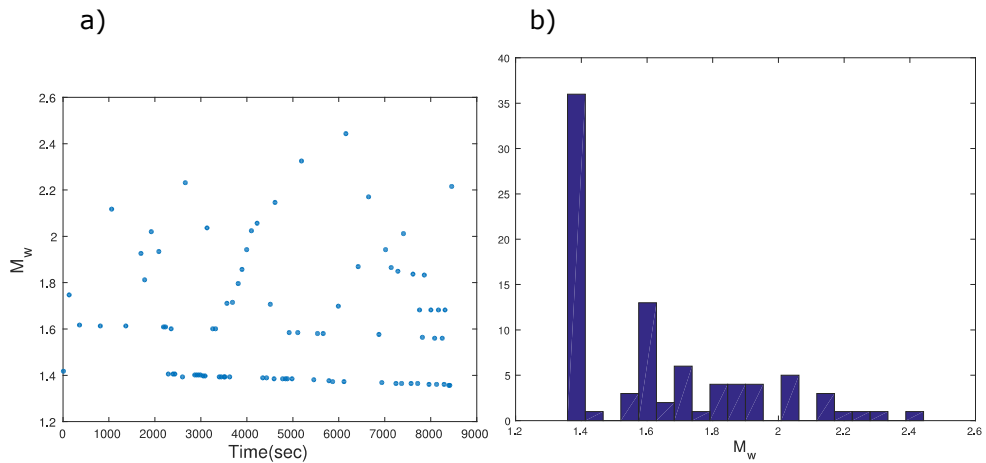


**Figure 8:** a) the moment magnitude with time; b) the distribution of induced seismicity.

### Timeline

During the last year, the focus was on developing a model for shear failure in fractures and the corresponding effect on fluid flow in a two-dimensional fractured reservoir scenario. The future steps will include extension of this coupled flow-mechanics simulator to three dimensional problem, to account for thermal cooling effect on the stress field in EGS, the hydro-fracturing effect and finally the comparison of simulation results with existing reservoir. The rough plan to achieve the above-mentioned key goals is the following:

- Development of 3-D flow-mechanics simulator within 3 months (Task 4.3)
- Addition of thermal effect into the mechanics within 3 months (Task 4.4)
- Hydrofracturing effect within 3 months (Task 4.4)
- Comparing simulation results with experimental results for existing reservoir data within 3 months (Tasks 4.2 and 4.5).

## **Deliverables**

Deb, Rajdeep, and Jenny, Patrick: Modeling of Failure Along Predefined Planes in Fractured Reservoir, *Proceedings*, 39th Workshop on Geothermal Reservoir Engineering, Stanford University, Stanford, California, February 24 - February 26, 2014 SGP-TR-202

Deb, Rajdeep, and Jenny, Patrick: Numerical Modeling of Flow Induced Shear Failure in Fractured Reservoirs, *Proceedings*, 40th Workshop on Geothermal Reservoir Engineering, Stanford University, Stanford, California, January 26 - January 28, 2014 SGP-TR-204

## 5. Geochemical effects on long-term permeability evolution & heat extraction (Module 5)

Dr. Thomas Driesner, (*Institute of Geochemistry and Petrology, ETH- ERDW*)  
 Dr. Julian Minde (*ETH-ERDW*)

### 5.1 Main scientific achievements and deliverables

Chemical reactions between the circulated fluid and the geothermal reservoir rocks can lead to mineral precipitation or dissolution, which (a) will affect the mechanical properties and hydraulic apertures of fractures, (b) result in reduction or enhancement of reservoir permeability, and (c) induce the formation of mineral scaling in the installations. All three factors affect reservoir performance and sustainability. As it is basically impossible to directly monitor where and how fast such reactions evolve in the reservoir, computer simulation is the primary tool to investigate them and provide information relevant for decision making in reservoir management. The "reactive transport simulation" method is the tool of choice, but its application to EGS has so far been hampered by technical limitations to represent discrete fracture networks in a porous rock matrix.

Task	Description	2013												2014 <i>today</i>												2015												2016			
		Ma	Ju	Ju	Au	Se	Oc	No	De	Ja	Fe	Ma	Ap	Ma	Ju	Ju	Au	Se	Oc	No	De	Ja	Fe	Ma	Ap	Ma	Ju	Ju	Au	Se	Oc	No	De	Ja	Fe	Ma	Ap				
		1	2	3	4	5	6	7	8	9	10	11	12	13	14	15	16	17	18	19	20	21	22	23	24	25	26	27	28	29	30	31	32	33	34	35	36				
5.1a	Code modifications	M/D5.1a																																							
5.1b	Small-scale reactive transport simulations									M/D 5.1b																															
5.1c	Exploring possibility of upscaling results													D 5.1c																											
5.2	Larger-scale simulation results																	M/D 5.2																							

Deliverables description	Status
D5.1a Adapt code to 3D simulations : Required input for other tasks	Delivered
D5.1b Small scale reactive transport simulations	Delivered
D5.1c Report: Parameterizations of simplified chemical models	Month 24
D5.2 Report: Larger-scale simulation results	Month 30
Milestones description	Accomplished
Completion of CSMP code modifications	Accomplished
Completion of small-scale reactive transport simulations	Month 36
Completion of thermo-hydraulic simulations using CSMP	

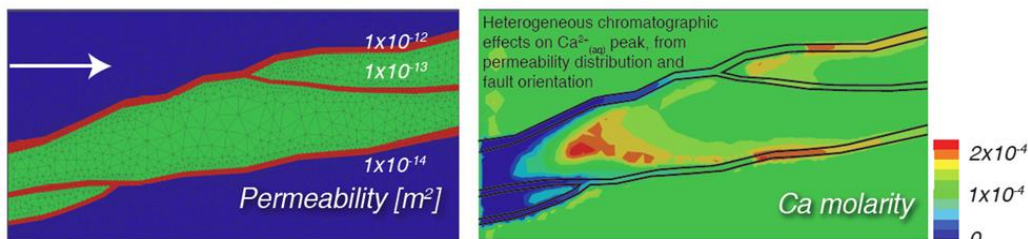


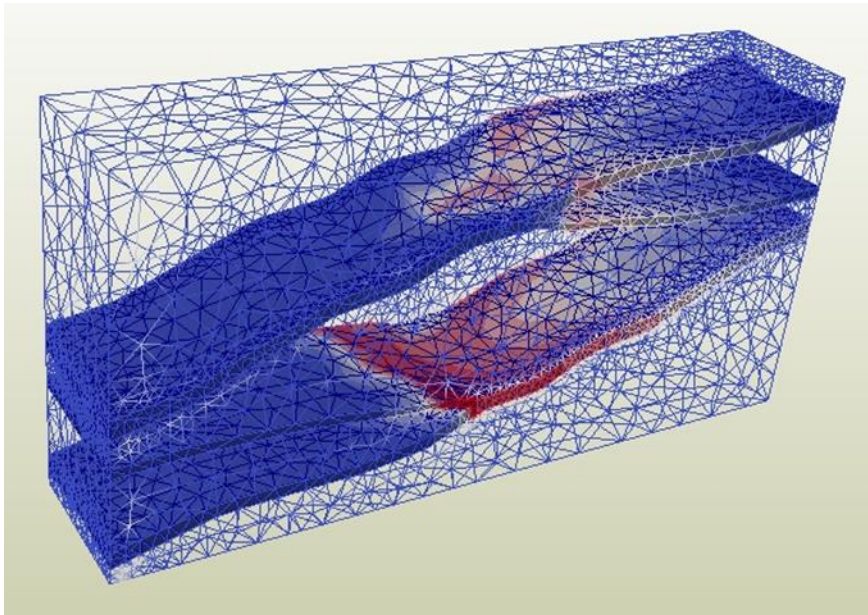
**Figure 9** Project status after the first GEOTHERM project. 2D reactive transport simulations of fluid-rock interaction in a fractured porous rock, showing the heterogeneous advancement of a reactive front, modified by chromatographic effects.

During the first GEOTHERM project, a prototype coupling between the CSMP++ fluid flow simulation platform (Matthai et al., 2007) and the GEMIPM2K (Kulik et al., 2004) chemical equilibration code was achieved and allowed 2D simulations of flow through porous matrix and fracture zones (Figure 9). Reconnaissance simulations indicated a strong dependence of the propagation of reaction fronts on the hydraulic characteristics of fracture zones and porous matrix. Module 5 has the aim to extend the cou-

pled code to 3D and apply it to realistic representations of EGS-like complex fracture networks in order to evaluate the possible impact of chemical fluid-rock interaction on the long-term performance of EGS. Such simulation capabilities would currently be unique.

### 5.1.1 Code Modification and Small Scale Reactive Transport Simulation (Tasks 5.1a, 5.1b)

Module 5 has so far focused on simulation code development and started working on applying the new code to actual research questions. The start of module 5 was hampered by the difficulty of finding suitable personnel. However, we were able to attract Dr. Julian Mindel from Montanuniversität Leoben, Austria, one of the most experienced developers of the CSMP++ code to work now 6 months per year for module 5, by this also enabling us to adapt to the constraints imposed by reduced third party funding. Dr. Mindel ported the previous code to the finite element / finite volume scheme of a fully revised new version of CSMP++ (Matthai et al, 2013) and coupled it to the new GEMIPM3K (Kulik et al., 2013) version of the chemical equilibration code. As a major step forward, the coupled code now works on arbitrary 3D geometries of fracture zones in a porous matrix, allowing us to simulate the effects of mineral dissolution, precipitation and reaction on the aperture distribution in an EGS-type reservoir and on the mineral load of the produced fluids (Figure 10). Preliminary simulations demonstrate the effects of fracture zone orientations relative to the pressure field and fracture zone intersections on the differential advance of reaction fronts.



Systematic simulations to explore these effects will be performed in the next reporting period.

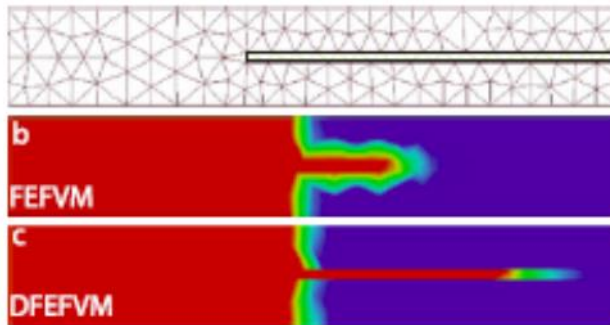
**Figure 10** Example of a reaction front (white to reddish colors) that migrates through two permeable fracture zones in a less permeable matrix. This rather simple test geometry was used to compare first 3D results to the previous 2D simulations from the GEOTHERM project (see Figure 9) but is already more complex than what can be resolved with standard tools used in geothermal industry.

Due to his intimate knowledge of the code, Dr. Mindel could achieve the milestones and deliverables in relatively short time. To complete task 5.1a (“Adapt code to 3D simulations”) the code was adapted to 3D simulations in the new CSMP++ version, which is an essential pre-requisite for the next tasks. In addition to the original plan, an interactive command line tool for setting up and running simulations was developed to speed up parameter studies.

The new code modules are now stored in the CSMP++ community’s main code repository (<http://csmpproject.unileoben.ac.at/index.php/csmpp>; repository access for registered users and developers only). The next semi-annual release of CSMP++ will make this functionality available to the users.

In terms of timeline the project is nearly perfectly on track. The first results of the project will be presented at The AGU Fall Meeting in December 2014. With Dr. Thomas Driesner and Dr. Julian Mindel two experienced CSMP++ developers work now part time on the project to be able to compensate for the reduced third party funding and late start. We have commenced the task 5.1b (“Small scale reactive transport simulations”) to start exploring the implications for EGS.

On a more technical side, we will test and compare the effect of various ways of representing fractures and fracture zones in irregular meshes: fractures and fracture zones of finite thickness with internally varying properties can be represented by layers of prism elements while thin fractures can be represented as lower dimensional (=2D) elements in the 3D model. A key step will be to make use of the "split node" capabilities of CSMP++ (Nick & Matthai, 2011) to maintain sharp interfaces at material boundaries (Figure 11).



represented as lower dimensional (=2D) elements in the 3D model. A key step will be to make use of the "split node" capabilities of CSMP++ (Nick & Matthai, 2011) to maintain sharp interfaces at material boundaries (Figure 11).

**Figure 11** From Nick & Matthai (2011), ability of CSMP++ to maintain sharp chemical interfaces along discretely represented fractures (bottom) compared to standard discretization (middle). Adapting this functionality to the reactive transport scheme of module 5 will result in a unique tool for numerical EGS simulations.

In a broader context, these efforts are embedded in the modeling activities of the new SCCER-SoE. A new working group of nearly ten researchers from PhD students to senior scientists will augment the simulation tools described in this report by thermo-hydro-mechanical couplings. To the best of our knowledge, the resulting combination of technical features will result in a unique tool for the geothermal simulation community.

## References

- Matthai S.K., Geiger S., Roberts S.G., Paluszny A., Belayneh M., Burri A., Mezentsev A., Lu H., Coumou D., Driesner T. and Heinrich C.A. (2007), In: *Structurally Complex Reservoirs* (S.J. Jolley, D. Barr, J.J. Walsh and R.J. Knipe, eds) Geological Society, London, Special Publications 292, 405-429.
- Kulik D., Berner U. and Curti, E. (2004) PSI Scientific Report 2003. Nuclear Energy and Safety, IV, 109-122.
- Matthai S.K. et al. (2012), ECMOR XIII, European Conf. Mathematics of Oil Recovery, Biarritz, France
- Kulik D.A., Wagner T., Dmytrieva S.V., Kosakowski G., Hingerl F.F., Chudnenko K.V., Berner U.R. (2013) *Computational Geosciences* 17,1-24.
- Nick H.M. and Matthai S.K. (2011), *Vadose Zone Journal* 299-312.

## 6. Geothermal energy usage in cities (Module 6)

Prof. Francois Marechal (*Industrial Energy Systems Laboratory, EPFL-IPESÉ*)  
 Stefano Moret (*EPFL-IPESÉ*); Mennon Ramannunui (*EPFL-IPESÉ*)  
 Prof. Liesse Laloui, Dr. Lauren Tacher (*Soil Mechanics Laboratory, EPFL-LMS*)  
 Dr. Peter Bayer (*Geological Institute, ETHZ-ERDW*)

### 6.1 Main scientific achievements and deliverables

The goal of the module is to complement the work already realized under GEOTHERM-1 by studying the integration of the conversion of geothermal energy from different depths and its usage in the energy system of cities. This concerns the development of a decision support tool, which includes geographic information (GIS) to geo-localize and characterize the demands and the geothermal resources:

- a database of energy conversion technologies for both heat and power production;
- a comprehensive thermodynamic and life cycle impact assessment tool of selected systems designs;
- a design tool based on optimization and process integration techniques to define the best energy conversion system in sizes and operating strategy;
- an analysis to assess the impact of the uncertain parameters on the system design decision.

Task	Description	2013			2014												2015				2016																	
		Ma	Ju	Ju	Ma	Ju	Au	Se	Oc	No	De	Ja	Fe	Ma	Ap	Ma	Ju	Au	Se	Oc	No	De	Ja	Fe	Ma	Ap												
		1	2	3	4	5	6	7	8	9	10	11	12	13	14	15	16	17	18	19	20	21	22	23	24	25	26	27	28	29	30	31	32	33	34	35	36	
6.1a	Characterization of energy services in cities: Methodol.																																					
6.1b	Validation by applying on test cases																																					
6.1c	Extrapolation to the major cities of Switzerland																																					
6.1d	Analysis of the non conventional heating																																					
6.2a	Geothermal resource characterization																																					
6.2b	Thermo-economic model of the geothermal resource harvesting																																					
6.3a	Characterization of the geological heat reservoir																																					
6.3b	Thermo-economic model of the heat storage options																																					
6.4	Energy conversion systems																																					
6.5a	Inventory analysis (LCI)																																					
6.5b	Integration of the inventories in the EGS module models																																					
6.5c	Impact assessment																																					
6.5d	Estimation of uncertainties for the optimization method																																					
6.5e	Interpretation methodology																																					
6.6a	System design using optimization techniques																																					
6.6b	Interpretation of the results																																					

Deliverables description	Status
D6.1a Report: Development of the methodology	Delivered
D6.1b Report & Database: Validation by applying on test cases	Month 24
D6.1c Report & Database: Extrapolation to the major cities of Switzerland	Month 36
D6.1d Report & Database: Non-conventional heating in cities and industrial parks	Month 36
D6.2a Report & Database: Geothermal resource characterization	Month 36
D6.2b Model: Thermo-economic model of the geothermal resource harvesting	Month 36
D6.3a Report & Database: Characterization of the geological heat reservoir	Month 36
D6.3b Model: Thermo-economic model of the heat storage options	Month 36
D6.4 Model: Energy conversion systems	Month 36
D6.5 Report & Database: Environmental impact assessment	Month 36
D6.6a Model: System design using optimization techniques	Month 36
D6.6b Report: Interpretation of the results	Month 36



### 6.1.1 Characterization of energy services in cities (Task 6.1)

(Contributor EPFL- IPESE)

Task **6.1a** has been completed with the definition of a general methodology to characterize energy services in cities based on the type and quality of available data (Figure 12). Various approaches and tools (ENERGIS, CitySim, etc.) in the literature have been reviewed in detail (F. Wolf et al., 2014). The key challenge has emerged to be the characterization of heating demand seasonal variations when only annual data are available or can be estimated. The methodology is being refined in Task **6.1b**. In this context it will be tested in the framework of a case study in the city of Lausanne. Energy signature and dynamic simulation approaches will be compared to measured data with the aim of refining the methodology, which could then be extended to other cities in Switzerland (Task **6.1c**). In the framework of this task, close collaboration has been established with various partners and stakeholders: the city of Lausanne, the CREM research center and the HES-SO Valais. Concerning non-conventional heating applications (Task **6.1d**), preliminary analyses are being performed concerning the use of geothermal heat in CO<sub>2</sub> capture processes and in combination with biomass resources.

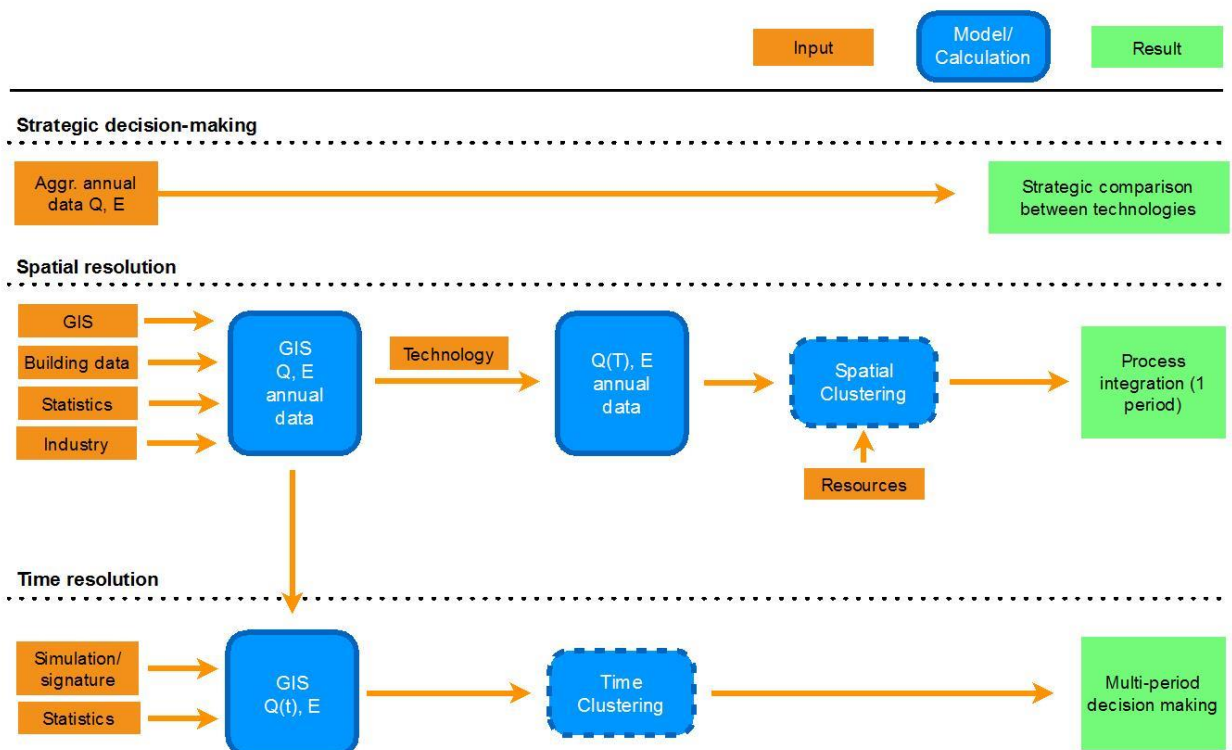


Figure 12 Overview of the methodology for the energy demand characterization (Task 6.1a)

### 6.1.2 Characterization of the geothermal resources, of the cold source and possible shallow storage (Tasks 6.2 & 6.3)

(Contributor EPFL-LMS)

The role of EPFL/LMS in this task is to produce a geological model of Lausanne city as an input to test the processes developed at EPFL/LENI. The model was finished and delivered at EPFL/LENI in August 2014. In 2015, our goal is to develop and implement a tool to assess the uncertainty on geological models. Hereunder is a brief description of the model.

A specificity of this model is to address both deep and shallow geological bodies, i.e., with a great level of detail in the superficial Quaternary deposits, while in depth direct knowledge is poor and structures probably rather smooth.

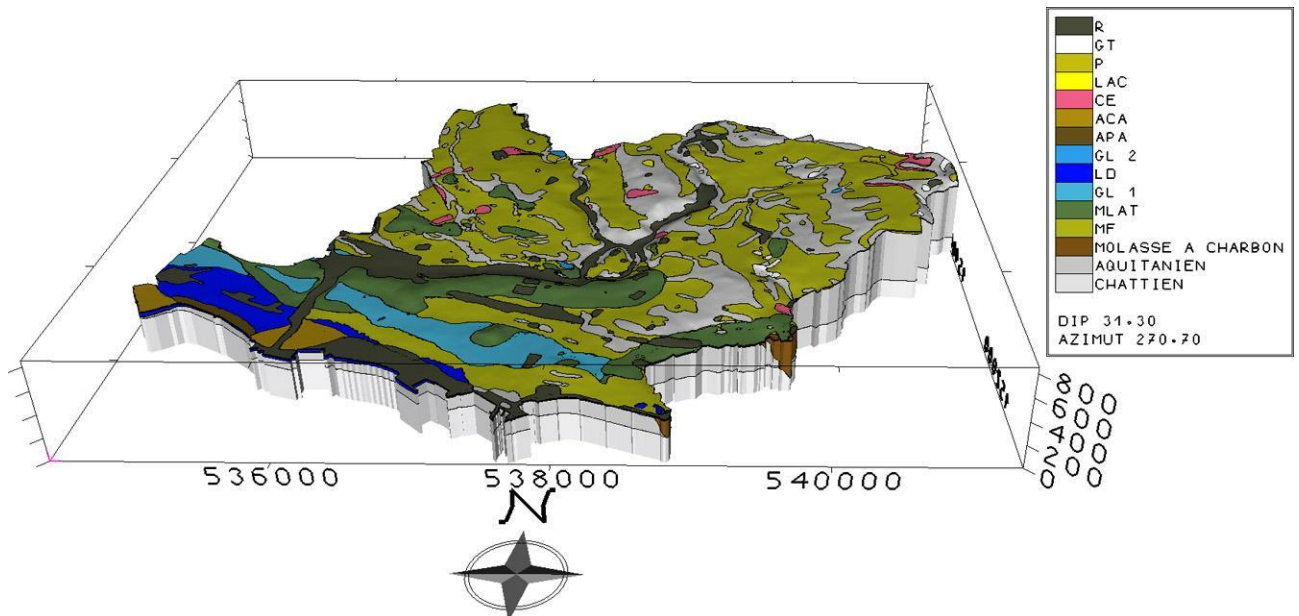


Figure 13 Lausanne shallow geological model

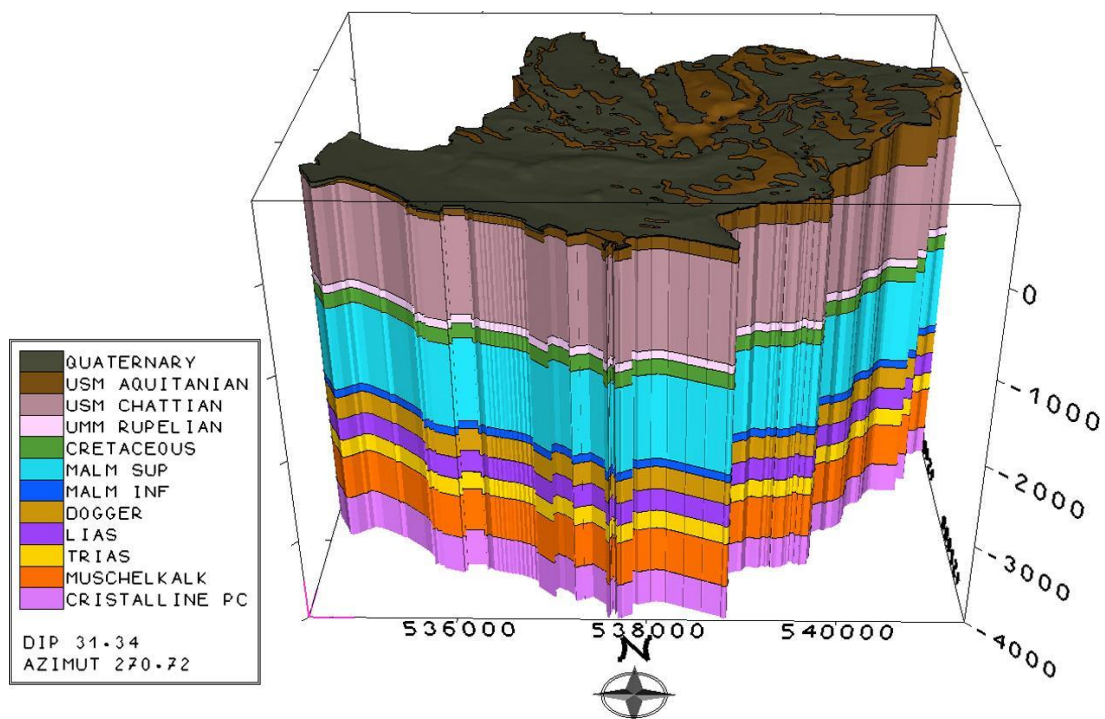
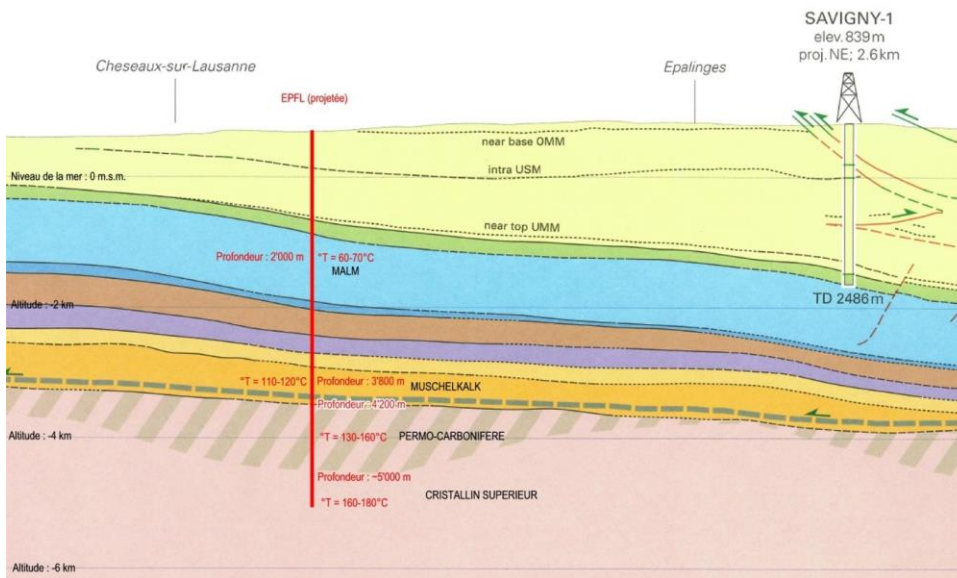


Figure 14 Lausanne deep stratigraphical model

In practice, two models were built. The first one details the Quaternary deposits and the upper molasse; its bottom is at 0 m a.s.l (Figure 13). The second model has its bottom at - 4000 m a.s.l. and all superficial deposits are grouped in a single formation named Quaternary (Figure 14).

- The base document for Quaternary shallow modeling is the geotypes map established by Etat de Vaud, Direction générale de l'environnement (DGE / DTE).
- To perform the deep geological assessment, the base document consulted is the Seismic Atlas of the Swiss Molasse Basin by Sommaruga et al., 2012.

To build the deep model, a typical stratigraphic column is issued from the Seismic Atlas of the Swiss Molasse Basin, Profile # 3 "Lac de Joux - Villeneuve" at Epalinges (Figure 15). At this place, the thicknesses were reported and used to draw the various interfaces below Lausanne. The consequence is that at the scale of Lausanne city, the thicknesses of the various layers are supposed constant.



The consequence is that at the scale of Lausanne city, the thicknesses of the various layers are supposed constant.

**Figure 15** Portion of Profile # 3 "Lac de Joux - Villeneuve" at Epalinges, Seismic Atlas of the Swiss Molasse Basin, 2012. In the Lausanne model, thicknesses were assessed at Epalinges. The EPFL site is also projected on the profile, showing assessed temperatures by the author. These supposed temperatures can be used as an estimate of the ones below Lausanne

The connection with the former shallow model is done at the so-called Intra USM1 interface, that we suppose to be the contact between the lower USM ( Chattian molasse) and upper USM ( Aquitanian molasse).

Table 4 Geological interfaces with approximate depths and thickness. Source: Seismic Atlas of the Swiss Molasse Basin, 2012. These thicknesses are used to prepare corresponding interfaces by isopachy based on the top of Chattian molasse, considered to be the Intra USM interface (e.g. Top UMM is a copy of Intra USM shifted 1100m downward).

Interface	Elevation (m a.s.l)	Thickness (m)
Topography	825	100
Base OMM	725	625
Intra USM	100	1100
Top UMM	-1000	100
Top Cretaceous	-1100	175
Top Malm > (incl. Oxfordian)	-1275	1000
Top Malm < (till Oxfordian)	-2275	100
Top Dogger	-2375	275
Top Lias	-2650	275
Top Trias >	-2925	225
Top Muschelkalk	-3150	550
Top crystalline or Permo-carb.	-3700	

1 USM: Lower fresh water Molasse, UMM Lower Marine Molasse, OMM: Upper marine Molasse

Potential aquifers are the following:

Potential aquifer	Rock type	Depth	Estimated température (geothermal gradient: 30°C/km)
Malm	Limestones, dolomites	ca. 1'800 – 2'200 m	60 – 70 °C
Muschelkalk (Trias)	Dolomitic limestones, gypse	ca. 3'700 – 3'900 m	110 – 120 °C
Permo-Carbonifère	Sandstones, conglomerates and schists	from ca. 4'200 m	130 – 160 °C
Cristalline	Gneiss, granites	> 4'200 m	130 – 160 °C and till 200°C

The Malm aquifer could be karstified in a part of its thickness (ca. 400 m). It is the target of several successful geothermal doublets in the Munich basin. The one of Muschelkalk has shown to be very productive in Riehen (20 l/s) and less productive in the Schlattigen (TG) borehole (6 to 8 l/s). Little is known about the Permo-Carboniferous. Its thickness could be over 1000m. The crystalline basement (granite or gneiss) is probably aquifer in its first 300 to 500 m, as shown by several drilling by NAGRA/CEDRA, as well as in the Basel borehole.

It is pointed out that the geological stratigraphy is rather well known thanks to seismic investigations for several decades. However, it is very difficult to deliver values of permeability in the aquifers due to the low level of knowledge concerning fracturation and karstification in the area.

### 6.1.3 Energy conversion systems (Task 6.4)

(Contributor LENI-EPFL)

A review of energy conversion system models (Task 6.4), mainly consisting in an update of the cost parameters, is under way. In this framework an active collaboration has successfully been put in place with the Tester group at Cornell University (USA).

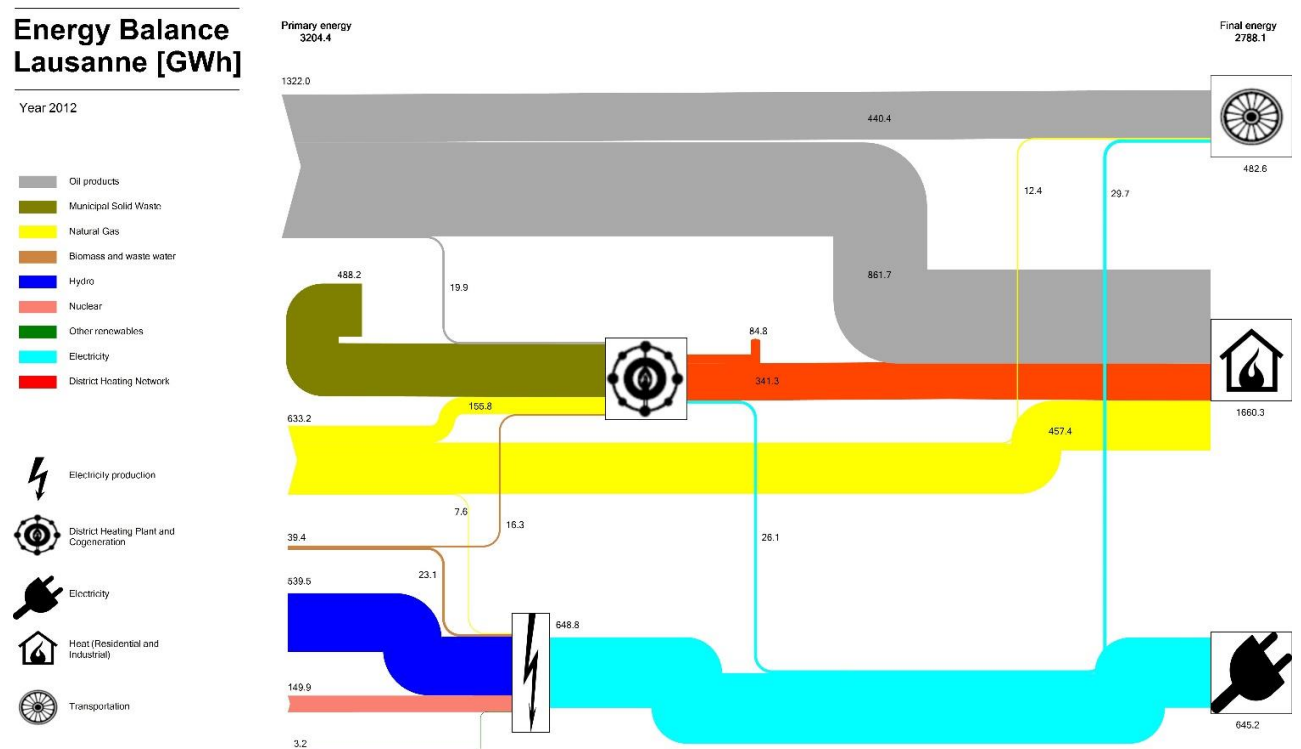


Figure 16 Sankey diagram representing energy flows in the city of Lausanne (2012)

The city of Lausanne is the urban system serving as case study for the test and refining of the developed methodologies. After the official definition of the collaboration with the city, sealed by the signature of a NDA, the first part of the work has mostly involved data collection and analysis. This has led to the possibility of getting an overall picture of the energy flows in the city, mapping the current situation (Figure 16). The city energy demand is mostly supplied by fossil fuels, and heating represents about 60% of the final energy consumption. A District Heating Network (DHN) satisfies about 20% of this demand. The key challenge and opportunity for geothermal energy is its integration in the DHN, which is planned to satisfy an increasing part of the heating demand in the next year. From the electricity production side, an opportunity in the Swiss context arises from the phasing out of nuclear power plants by 2034.

#### 6.1.4 Environmental impact assessment (Task 6.5)

(Contributor ETHZ\_ERDW)

In order to investigate the environmental performance of Enhanced Geothermal Systems (EGS) a life-cycle assessment (LCA) methodology is applied, which accounts for all environmental impacts throughout the life-cycle of a geothermal power plant. The procedure of an LCA is prescribed in given standards (i.e. ISO 14040, ISO 14 044), which defines several stages within the LCA. The first step of this procedure is the goal and scope definition. For the investigation within the scope of the GEOTHERM project, the geographical reference was set to Switzerland and the time reference was defined to be the year 2010 according to the date of the employed Ecoinvent 2.2 database. All environmental effects during the overall life-cycle (i.e. from "cradle-to-grave") were then analyzed in reference to the functional unit. To enable comparison to other energy technologies the functional unit was defined as one kWh net power at the plant.

##### Task 6.5a: Life-cycle Inventory Analysis (LCIA)

Central part of this task was the setup of the life-cycle inventory. In this step of the LCA methodology all mass and energy flows that occur during the life-cycle of an EGS power plant were quantified and related to the functional unit. All inputs and outputs were assigned to the individual life stages in which they occur to investigate to which amount the stages of construction, operation and decommissioning contribute to the life time environmental effects. As previous studies suggested, the construction phase causes a rather large share of the overall environmental impacts (Frick et al., 2010; Lacirignola & Blanc, 2013). The inventory of this life stage was further divided into surface and subsurface construction. Based on this structure, an LCA model was set up using the commercial software SimaPro7. Specific plant parameters, such as reservoir temperature and borehole depth, were included as variable parameters. Thus, the model can be easily adapted to different plant configurations or reservoir scenarios. This site-specific information was derived from reports of (mostly planned) EGS projects, for example, in Basel and St. Gallen (see Table 5). Life-cycle information on general components of the power plants, such as heat exchangers or pipelines, was obtained by an extensive literature review of previous LCA studies (Frick et al., 2010; Lacirignola et al., 2013). Data on common products, such as diesel or steel, and processes, e.g. transportation, was taken from the Ecoinvent 2.2 database.

**Table 5** Excerpt of the site-specific reservoir characteristics and power plant parameters assigned for the LCA model of the planned EGS in Basel and St.Gallen.

Parameter	Basel	St.Gallen
Number of boreholes	3	2
Borehole depth [m]	5000	4450
Projected lifetime [years]	30	30
Geothermal fluid temperature at production[°C]	190	145
Geothermal fluid temperature at reinjection[°C]	70	70
Geothermal fluid flow [m <sup>3</sup> /h]	288	180
Conversion efficiency of ORC [-]	0.132	0.104
Power capacity [MW]	3.0	4.5

**Task 6.5c: Impact assessment**

Following the standard LCA procedure, the life time emissions of the EGS plant were quantified and evaluated with respect to different impact indicators, such as greenhouse gas (GHG) emissions and cumulative energy demand (CED). Figure 17 shows a simplified flow chart of the LCA model of the planned EGS in St. Gallen with the life time GHG emissions adding up to 24.8 gCO<sub>2</sub>-eq./kWh. The thickness of the red arrows in the flow chart indicates the magnitude of the environmental impact corresponding to the individual life stages and components of the plant. The majority of the life-time GHG emissions are obviously caused by the construction of the geothermal wells, in particular by the use of steel for the casing of the boreholes.

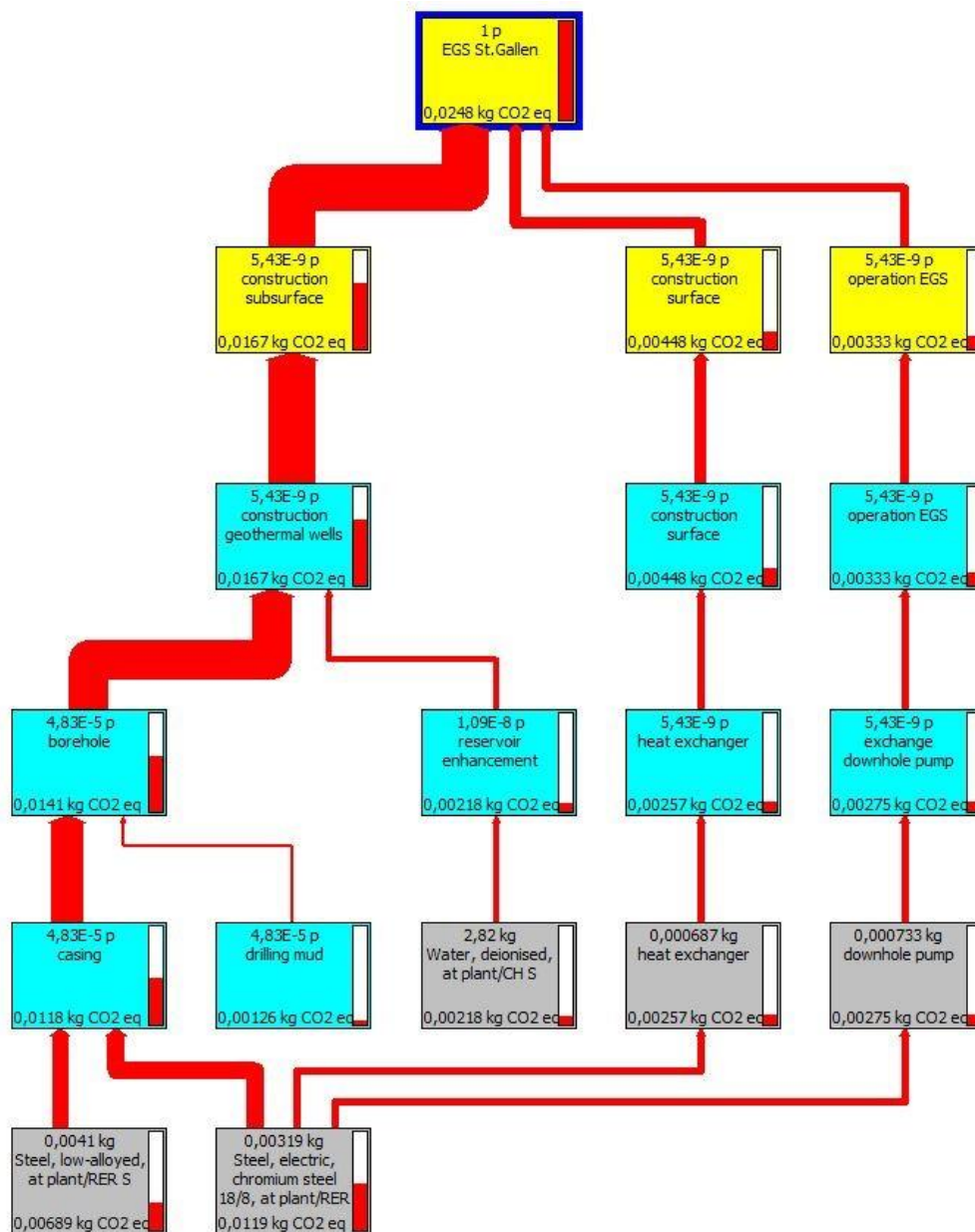


**Figure 17:** Simplified flow chart of the LCA model of the planned EGS in St. Gallen showing processes that contribute more than 5% to the overall life time CO<sub>2</sub>-equivalent GHG emissions per produced kWh net energy. The thickness of the red arrows indicates the share of the individual components in the life-time emissions.

A detailed analysis of previous LCA studies of EGS in Germany (Frick et al., 2010) and France (Lacirignola & Blanc, 2013) showed that the environmental impact of the investigated Swiss projects is comparably low due to the use of environmentally friendly drilling technologies. While the geothermal wells described in previous LCA studies were constructed by diesel driven drilling rigs, electricity driven rigs were

used in St. Gallen and Basel. Because of the large percentage of low-carbon energy production technologies in Switzerland, the environmental impact of EGS is also significantly lower.

The second part of task 6.5d was the comparison of the environmental performance of EGS compared to other renewables as well as conventional energy technologies. An extensive literature was carried out to collect data on the environmental impacts of existing power generation technologies from previous LCA studies (e.g. Pehnt, 2006; Sullivan et al., 2010). Figure 18 shows the life-time GHG emissions of a selection of the investigated technologies. The emissions of EGS power plants are in the same order of magnitude as other renewable energies, such as hydro or solar power. Compared to power production from fossil fuels, such as natural gas or coal, the environmental performance of EGS plants is significantly better. However, it should be considered that the ranking of the technologies in Figure 18 could change considerably, when other environmental effects, such as the depletion of finite resources or the acidification potential, are considered instead of global warming.

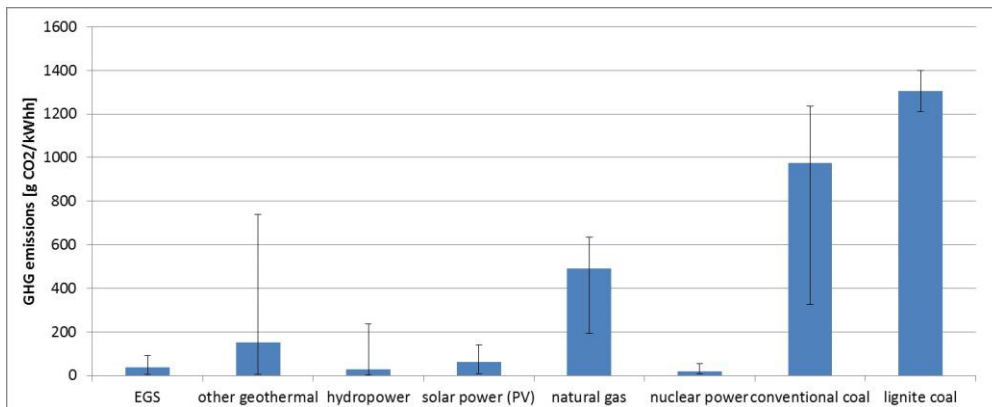
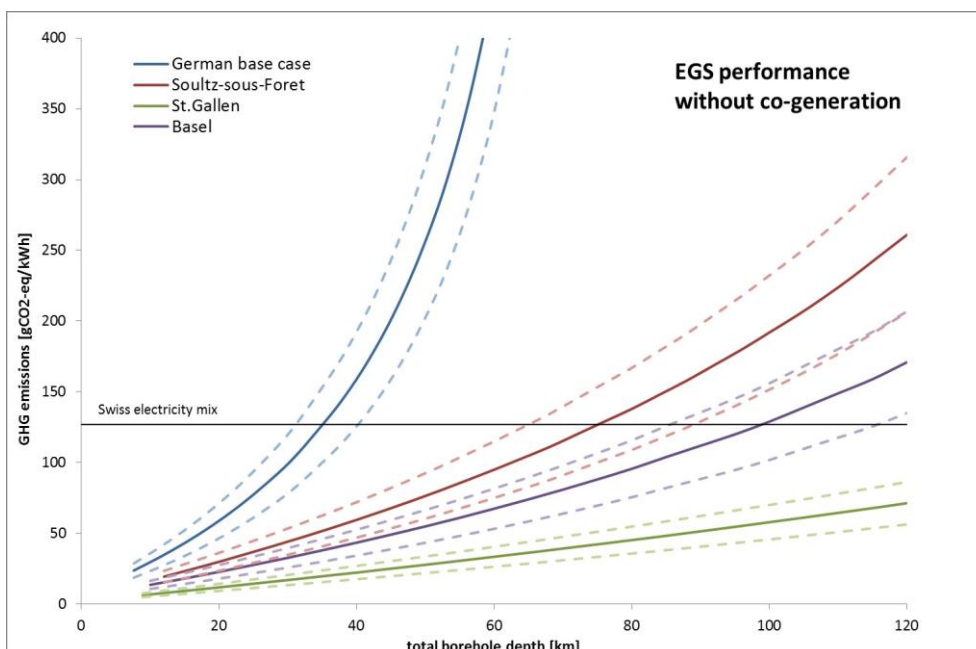


**Figure 18** Life-time green-house gas emissions by EGS power plants and other energy production technologies.

**Task 6.5d: Characterization of the uncertainties**

Based on previous LCA studies and reports from planned or existing geothermal projects it can be stated that the largest uncertainties in such projects are related to the geological site conditions. Due to the inaccuracy of the prediction methods the expected reservoir characteristics are not always encountered. In case of an overestimation of the reservoir temperature or geothermal flow rate, this often results in the need of additional or deeper geothermal wells. As mentioned above the construction of the boreholes causes the major part of the life-time GHG emissions. Thus, the drilling of additional boreholes can impair the environmental performance of an EGS power plant significantly. Figure 19 shows the life-time GHG emissions of three proposed EGS in Switzerland and Germany (Frick et al., 2010) and the existing power plant in Soultz-sous-Foret (Lacirignola & Blanc, 2013) as a function of the total borehole depth, i.e., the sum of the depth of all drilled wells. Depending on the site-specific amount of energy and materials that are needed to construct these wells, the curves exhibit different ascending slopes with increasing depth. Due to the efficient drilling at the sites of Basel and St. Gallen, these two EGS plants show again lower life-time GHG emissions than the other power plants.



Due to the efficient drilling at the sites of Basel and St. Gallen, these two EGS plants show again lower life-time GHG emissions than the other power plants.

**Figure 19** Life time GHG emissions from several EGS power plants as a function of the total borehole depth. As a threshold for a competitive environmental performance the mean GHG emissions of the Swiss electricity mix are also shown.

Figure 19 also shows the mean value for the amount of GHG emissions released per kWh of electricity produced in Switzerland. This value can be interpreted as a threshold for the environmental competitiveness for EGS systems. Accordingly, for the Basel case the tremendous amount of approx. 100 km of total borehole meters could be drilled before the environmental performance of the EGS would be equal to the current electricity mix. With an individual borehole depth of 5 km this value would allow for 20 boreholes to be drilled during the estimated life-time of 30 years.

For the future work on this task, it is planned to additionally include the uncertainties of the basic parameters taken from the Ecoinvent database into the LCA results. Ranges for these parameters are contained in the database and will be implemented in the LCA models by performing a Monte Carlo simulation.

#### Task 6.5e: Interpretation methodology

This task will be assessed in the near future.

### **6.1.5 Energy system design (Task 6.6)**

*(Contributor EPFL-LENI)*

For Task 6.6a a first application of optimization has been performed for the city of Lausanne by developing a simplified model of the Lausanne urban energy system and evaluating the integration of the optimal EGS configurations emerged from the results of GEOTHERM-1. Preliminary results have underlined how the high temperature of the city's DHN is a key variable for the feasibility of the deployment of EGS in the context of Lausanne. Only-heating and cogeneration options appear to be the most promising if CO<sub>2</sub> emission reduction is the target, as the direct competitor for electricity production for the city is hydro power. A more detailed study is being realized by integrating the updated EGS models.

The integration of geothermal energy in the overall scheme of the Swiss energy system finds application in the development of the online platform [swiss-energyscope.ch](http://www.swiss-energyscope.ch), a tool with the goal of spreading energy literacy and aiding decision-making (Moret et al., 2014a).

In line with previous highlighted results, a preliminary work has been developed on the classification of uncertainty and robust optimization for decision-making in energy systems. Preliminary results suggest that the consideration of the impact of the uncertainty could be a key enabler for a wider deployment of renewable energy technologies (Moret et al., 2014b).

#### **Timeline report**

The project is proceeding according to the schedule

#### **Deliverables**

##### – Task 6.1

Refinement of DHW demand modelling in EnerGIS. F. Wolf, N. Schüler, F. Maréchal (dirs.). EPFL semester project report, 2014.

##### – Task 6.6

S. Moret, V. Codina Gironès, F. Maréchal and D. Favrat. *Swiss-energyscope.ch: a Platform to Widely Spread Energy Literacy and Aid Decision-making*. (2014a) PRES 2014 - 17th Conference Process Integration, Modelling and Optimisation for Energy Saving and Pollution Reduction, Prague, Czech Republic, 2014. The developed platform will be publicly available in January 2015 at the link <http://www.swiss-energyscope.ch>.

S. Moret, M. Bierlaire and F. Maréchal. *Robust optimization for strategic energy planning*. (2014b) 1st European Conference on Stochastic Programming and Energy Applications (EuroCSP 2014), Paris, France, 2014.



## References

Frick S, Kaltschmitt M, Schröder G. Life cycle assessment of geothermal binary power plants using enhanced low-temperature reservoirs. *Energy*. 2010;35:2281-94.

Lacirignola M, Blanc I. Environmental analysis of practical design options for enhanced geothermal systems (EGS) through life-cycle assessment. *Renew Energy*. 2013;50:901-14.

Pehnt M. Dynamic life cycle assessment (LCA) of renewable energy technologies. *Renew Energy*. 2006;31:55-71.

Sullivan JL, Clark CE, Han MWJ. Life-cycle analysis results of geothermal systems in comparison to other power systems. Argonne National Laboratory, Energy Systems Division, US Department of Energy; 2010.